Published in final edited form as:
J Comp Neurol. 2015 February 15; 523(3): 359–380. doi:10.1002/cne.23664.

Conserved expression of the GPR151 receptor in habenular axonal projections of vertebrates

Jonas Broms[1,*], **Beatriz Antolin-Fontes**[2,*], **Anders Tingström**[1,#], and **Ines Ibañez-Tallon**[2,#]

[1]Psychiatric Neuromodulation Unit, Clinical Sciences, Lund University, Lund, Sweden

[2]Laboratory of Molecular Biology, The Rockefeller University, New York, U.S.A

Abstract

The habenula is a phylogenetically conserved brain structure in the epithalamus. It is a major node in the information flow between fronto-limbic brain regions and monoaminergic brainstem nuclei, thus anatomically and functionally ideally positioned to regulate emotional, motivational and cognitive behaviors. Consequently, the habenula may be critically important in the pathophysiology of psychiatric disorders such as addiction and depression. Here we investigated the expression pattern of GPR151, a G coupled-protein receptor (GPCR), whose mRNA has been identified as highly and specifically enriched in habenular neurons by in situ hybridization and Translating Ribosome Affinity Purification (TRAP). In the present immunohistochemical study we demonstrate a pronounced and highly specific expression of the GPR151 protein in the medial and lateral habenula of rodent brain. Specific expression was also seen in efferent habenular fibers projecting to the interpeduncular nucleus, the rostromedial tegmental area, the rhabdoid nucleus, the mesencephalic raphe nuclei and the dorsal tegmental nucleus. Using confocal microscopy and quantitative colocalization analysis we found that GPR151 expressing axons and terminals overlap with cholinergic, substance P-ergic and glutamatergic markers. Virtually identical expression pattern was observed in rat, mouse and zebrafish brains. Our data demonstrate that GPR151 is highly conserved, specific for a subdivision of the habenular neurocircuitry, and constitutes a promising novel target for psychiatric drug development.

Keywords

G protein-coupled receptor; fasciculus retroflexus; interpeduncular nucleus; rostromedial tegmental nucleus; rhabdoid nnucleus; raphe nucleus; MGI_MGI:3606630; RGD_737929; ZIRC_ZL1; AB_10743815; AB_10608138; AB_307210; AB_887876; AB_887878; AB_887883;

[#]Corresponding authors: Anders Tingström, M.D., Ph.D., Psychiatric Neuromodulation Unit, Biomedical Center, D11, Klinikgatan 30, 222 42 Lund, Sweden, anders.tingstrom@med.lu.se, Phone: +46-46-2220611. Ines Ibañez-Tallon, Ph.D., Laboratory of Molecular Biology, The Rockefeller University, 1230 York Avenue, Box 260, New York, NY 10065, USA, iibanez@rockefeller.edu, Phone: 1-212-327-7989.
[*]These authors contributed equally to this work

CONFLICT OF INTEREST STATEMENT
The authors declare no conflicts of interest.

ROLE OF AUTHORS
All authors had full access to all the data in the study and take responsibility for the integrity and presentation of the data. Study concept and design: AT and IIT. Acquisition of data: JB, BAF. Analysis and interpretation of data: JB, BAF, AT, IIT. Writing of the manuscript: JB, BAF, AT, IIT. Conceptualization and critical revision of the manuscript for intellectual content: AT, IIT. Obtained funding: AT, IIT. Study supervision: AT, IIT.

AB_887884; AB_2079751; AB_10123643; AB_477560; AB_261587; AB_90754; AB_572266; AB_628299; SciRes_000137

INTRODUCTION

The habenula is an ancient, highly conserved brain structure present throughout the vertebrate lineage. The habenula is a bilateral diencephalic structure that modulates brainstem monoaminergic and cholinoreceptive nuclei (Lecourtier and Kelly, 2007; Bianco and Wilson, 2009). In lower vertebrates (such as fish and amphibians) the habenula is asymmetric. In contrast, the mammalian habenula shows no lateralization. It is divided in medial (MHb) and lateral (LHb) nuclei that are readily distinguishable in Nissl preparations. In addition, as many as 15 subnuclei have been described using ultrastructural, morphological and cytochemical criteria (Andres et al., 1999; Geisler et al., 2003; Aizawa et al., 2012; Wagner et al., 2014). The habenula is thus a highly heterogeneous structure, and this is also reflected by its diverse connectivity. The habenula receives inputs primarily via the stria medullaris and sends outputs via the fasciculus retroflexus. The MHb receives afferents from the septum and the diagonal band of Broca and projects to the interpeduncular nucleus (IPN) (Herkenham and Nauta, 1977; 1979), while the LHb receives input from large portions of the ventral forebrain, including the lateral preoptic area, lateral hypothalamus and basal ganglia as well as the serotonergic dorsal raphe and the dopaminergic ventral tegmental area (VTA) (Herkenham and Nauta, 1977; Sim and Joseph, 1993). In turn, the LHb projects mainly to the VTA, the median and dorsal raphe, and the recently described rostromedial tegmental nucleus (RMTg) (Herkenham and Nauta, 1979; Jhou et al., 2009b; Kim, 2009).

The behavioral contributions of the LHb and MHb have traditionally been reported as segregated, despite the fact that these nuclei are adjacent to each other and that intra-habenular connectivity has been described (Kim and Chang, 2005). The MHb and its major target, the IPN, have emerged as key regions in the regulation of nicotine consumption and withdrawal (Fowler et al., 2011; Frahm et al., 2011; Salas et al., 2009). The MHb shows the highest concentration of nicotinic acetylcholine receptors (nAChRs) in the brain (90–100% of the neurons in the MHb express α3, α4, β2, β3 or β4 nAChRs) (Görlich et al., 2013; Hsu et al., 2013; Sheffield et al., 2000). Importantly genetic variants in the *CHRNA5-CHRNA3-CHRNB4* gene cluster encoding α5, α3 and β4 nAChR subunits have been linked to nicotine dependence and smoking related diseases in humans (Berrettini et al., 2008; Bierut et al., 2008; Lips et al., 2010; Liu JZ et al., 2010; Ware et al., 2011). Functional studies have shown that α5 and β4 nAChRs in the MHb-IPN pathway regulate nicotine intake and withdrawal (Fowler et al., 2011, Frahm et al., 2011, Zhao-Shea et al., 2013) and that MHb neurons display spontaneous phasic activity that is enhanced upon nicotine withdrawal (Görlich et al., 2013).

On the other hand the LHb has been shown to play a crucial role in negative reward and decision-making (Hikosaka, 2010; Stopper and Floresco, 2013). Phasic activation of LHb neurons occurs during aversive stimulation or when a less-than-expected reward is presented (Matsumoto and Hikosaka, 2007; 2009). When unexpected negative events occur, activation of LHb causes inhibition of dopaminergic neurons in the VTA. This inhibition, mediated

mainly via a GABAergic relay in the RMTg, gives rise to the reward-prediction error response of VTA neurons (Balcita-Pedicino et al., 2011). LHb neurons also display slow, tonic responses encoding temporal proximity to future rewards (Bromberg-Martin et al., 2010). Optogenetic stimulation of excitatory synapses in the LHb, as well as stimulation of axon terminals of LHb neurons in the RMTg, produce an avoidance response (Shabel et al., 2012; Stamatakis and Stuber, 2012). Investigations of human brain activity using fMRI have found increased BOLD responses in the habenula to negative feedback and negative reward prediction error (Ullsperger and Cramon, 2003; Salas et al., 2010) as well as when cues associated with painful stimulation are presented (Lawson et al., 2014). Based on these findings, it has been proposed that the LHb does not merely encode disappointment, but that it provides information about cost and uncertainty in order to facilitate optimal decision-making and learning (Stopper and Floresco, 2013).

Both the LHb and MHb show reduced volume in people affected with depression (Ranft et al., 2010), thus implicating both nuclei in the pathophysiology of this disorder. Serotonergic neurons in the dorsal raphe, known to be involved in depression, are inhibited by stimulation of the habenula (Wang and Aghajanian, 1977; Reisine et al., 1982; Park, 1987). In agreement, increased LHb metabolism and reduced brain serotonin levels have been observed in several animal models of depression. This effect can be reversed with antidepressant drugs (Caldecott-Hazard et al., 1988; Shumake and Gonzalez-Lima, 2013) or lesions of the LHb (Yang et al., 2008). In fact, inactivation of the habenula by deep brain stimulation has been used in the treatment of major depressive disorder (Sartorius and Henn, 2007; Sartorius et al., 2010). Moreover, neuroimaging studies have identified heightened habenula activity in depressed patients (Morris et al., 1999; Roiser et al., 2009). However, determining the specific functional contribution of MHb versus LHb in human in vivo studies will require higher fMRI resolution than the currently commonly used 7 Tesla scanners allow for (Viswanath et al., 2013).

One gene that has been found to be highly expressed in both the MHb and the LHb is *GPR151* whose mRNA has been detected by in situ hybridization in the cell bodies of habenular neurons in the ventral MHb and in sparse neurons of the LHb (Berthold et al., 2003; Aizawa et al., 2012; Quina et al., 2009). GPR151, also known as PGR7, GALR4, GPCR-2037 and GALRL, belongs to the A type of G protein-coupled receptor (GPCR) and shows the highest homology to the galanin receptors 2 and 3 but responds only very weakly to the neuropeptide galanin (Ignatov et al., 2004). To this date, no endogenous or synthetic ligand for this receptor has been reported and its function is still largely unknown. The *GPR151* gene is conserved in mammals (~83% identity in human versus rodent and ~89% in rat versus mouse) and has orthologs in chicken and zebrafish (NCBI HomoloGene). The zebrafish genome contains two nearly identical copies of the *probable gpr151-like* gene (LOC100538082 and LOC565170), which share homology with human *GPR151* (54% DNA sequence identity). While the in situ hybridization mRNA pattern of *Gpr151* has been reported in rodents (Berthold et al., 2003, Aizawa et al., 2012, Quina et al., 2003) and Translating Ribosome Affinity Purification (TRAP) assay, identified *Gpr151* mRNA as highly and specifically enriched in mouse habenular neurons (Görlich et al., 2013), no studies have addressed the localization of the GPR151 receptor protein.

The present study therefore sought to investigate the protein expression pattern of GPR151 in rats, mice and zebrafish. Given the homologous organization of habenular subnuclei between mice and rat (Wagner et al., 2014), and the similar habenular neurocircuitry in fish (Amo et al., 2010), we compared the GPR151 immunoreactivity between these species, to determine whether GPR151 could be used as a marker for a conserved population of medial and lateral habenular neurons, that could further facilitate functional studies in all three model organisms. In order to characterize the GPR151 expressing neurons we used a combination of markers for known habenular neurotransmitters such as acetylcholine, substance P and glutamate, as well as markers for dopamine and serotonin to identify monoaminergic neuronal populations innervated by GPR151 positive projections.

MATERIALS AND METHODS

Animals

Mice and rats were housed with *ad libitum* access to standard lab chow and water in a room air conditioned at 22°C–23°C with a standard 12 hr light/dark cycle (lights on 7:00 am, off 7:00 pm), with a maximum of five mice or three rats per cage. GPR151 knockout mice ($GPR151^{tm1Dgen}$, RRID:MGI_MGI:3606630), where a *lacZ* reporter gene was inserted in place of the *Gpr151* exon, were obtained from Deltagen. They were backcrossed to C57BL/6J for eight generations. Six wild type C57BL/6J mice (The Jackson Laboratory, RRID:IMSR_JAX:000664), three $Gpr151^{-/-}$ mice and six Crl:WI Wistar rats (Charles River, Germany, RRID:RGD_737929) aged 8–12 weeks were used for experiments and were perfused between 10am and 2pm.

Fixation of mouse and rat brain tissue

The animals were deeply anesthetized by injecting an overdose of pentobarbital and perfused transcardially with 100 ml of cold isotonic NaCl solution (0.9%) followed by 200 ml of cold sodium phosphate buffered saline (PBS) containing 4% paraformaldehyde (PFA). The brains were then dissected and post fixed in 4% PFA for 24 hours at 4°C. A shorter post fixation time of 2 hours yielded uneven and weak immunostaining, especially in rat tissue. After post fixation, the brains were immersed in sucrose solution (25% in PBS) at 4°C for 2–3 days until equilibration had occurred (i.e. the brains sank to the bottom of the vial). The brains were sectioned in 40 μm sections using a sliding microtome (Thermo Scientific HM450), cryoprotected in antifreeze solution (30% glycerol, 30% ethylene glycol, 40% 0.5M PBS), and stored at −20°C until commencing immunohistochemistry.

Immunohistochemistry of mouse and rat sections

After rinsing in sodium phosphate buffered saline solution (PBS), free-floating brain sections were blocked in PBS containing normal serum (10% in mouse, 5% in rat) and 0.3% TritonX-100 for 1 hour. The normal serum matched the species in which the secondary antibodies were raised. Sections were then incubated overnight at 4°C with primary antibodies (Table 1) diluted in blocking solution. Subsequently, sections were washed with PBS and incubated for 2 hours at room temperature with secondary antibodies (Table 2). Sections were then washed twice for 15 minutes in PBS and counterstained with the nuclear stain DAPI at 1 μg/ml in PBS for 10 minutes. The sections were then mounted on Superfrost

Plus glass (Menzel-Gläser, Germany) and coverslipped with ImmuMount™ (Thermo Scientific).

For visualization of immunoreactivity for light microscopy, brain sections were incubated with a biotinylated anti-mouse secondary antibody made in horse (Vector Laboratories), followed by incubation with avidin-biotin-peroxidase complex (diluted 1:125 in PBS) (VECTASTAIN Elite ABC Kit, Vector Laboratories) and 3,3′-diaminobenzidine (DAB). Following the DAB reaction, sections were mounted, dehydrated in increasing concentrations of ethanol followed by xylene and finally coverslipped with DPX (Fisher Scientific).

The primary antibodies used in the experiment are listed in Table 1. When using VGLUT1 and VGLUT2 antibodies, TritonX-100 was omitted in order to preserve synaptic membranes. Heat mediated antigen retrieval, 15 minutes at 95°C in citric acid (pH 6.0), was performed prior to incubation with the ChAT antibody to enhance immunostaining.

Confocal fluorescent images were acquired with a Zeiss LSM700 confocal microscope. Brightness and contrast of the images was adjusted with Adobe Photoshop CS6.

Preparation of zebrafish brain tissue

Two adult zebrafish (7 months old, AB strain, RRID:ZIRC_ZL1) were rapidly chilled in ice cold water and subsequently immersed in PFA solution (4% in PBS) for 24 hours. The brains were then dissected and equilibrated in sucrose (20% in PBS). Subsequently, the brains were incubated in PBS containing 7.5% gelatin and 20% sucrose at 37°C for 2 hours. The brains were then put in to fresh gelatin-sucrose molds and cut into blocks. The blocks were cut in 14 μm transverse sections on a cryomicrotome and mounted on Superfrost Plus glass (Menzel-Gläser, Germany). Immunohistochemistry was performed as for mouse and rat sections except that incubation with GPR151 antibodies was performed directly on the glass instead of free-floating. Two polyclonal antibodies (raised in mouse and rabbit) against human GPR151 were used (described below).

Colocalization analysis

Images that were used for colocalization analysis were acquired with a 63x oil immersion objective on a Zeiss LSM700 confocal microscope. The detection pinhole was set to 1 Airy unit in order to maximize signal-to-noise. The channels where captured in sequence to minimize the risk of bleed-through. The intensity gain was adjusted for each channel before capture in order to avoid saturated pixels, and the intensity range of the images was left untouched to preserve linearity. Colocalization analysis was performed with the Coloc 2 plugin in the Fiji image processing package (v. 1.48, RRID:SciRes_000137). Background was eliminated by median subtraction (Dunn et al., 2011). Manders' colocalization coefficients, M1 and M2, which are proportional to the number of colocalizing pixels in each channel relative to the total number of pixels in that channel were calculated (Manders et al., 1994). M1 or M2 > 0.55 indicates colocalization (Zinchuk and Grossenbacher-Zinchuk, 2014). In the present study, only M1 is presented and refers to the proportion of pixels with Gpr151 immunoreactivity that colocalize with a second marker. Costes' test for statistical significance was used to determine that the colocalization coefficients obtained

where not due to random effects (Costes et. al., 2004). In the test, one channel is scrambled repeatedly (n=100) and correlated with the other channel, which results in a Costes' P-value where P is the proportion of random images that are less correlated than the original. A P-value > 0.95 indicates statistically significant correlation.

Antibody characterization

The antibodies used in the study are indicated below. Concentrations for optimal signal-to-noise ratio were determined for each antibody based on literature and serial dilution of the antibody. In all preparations, some sections were prepared identically except for omitting the primary antibody in order to ensure that the observed signal was not due to non-specific binding of the secondary antibody. Working concentrations (for purified antibodies) or dilutions (for non-purified antibodies) of primary antibodies are provided in Table 1.

1. Rabbit GPR151 polyclonal antibody (SAB4500418, Sigma-Aldrich) is raised against a synthetic peptide containing amino acids 370–419 (*EKEKPSSPSSGKGKTEKAEIPILPDVEQFWHERDTVPSVQDNDPIPWEHEDQETGEGVK)* of the C-terminal of human GPR151. It recognizes a single band of 46 kDa on western blots of K562 cell lysate. The specificity was confirmed by pre-adsorption with the immunogen peptide (according to manufacturer's technical information). Antibody specificity was in the present study verified using *Gpr151*$^{-/-}$ mice (see below).
2. Mouse GPR151 polyclonal antibody (SAB1402000, Sigma-Aldrich) is raised against full-length human GPR151 protein. Western blots of GPR151 transfected HEK293T lysate shows a band at ~46 kDa, which was not present in lysate of non-transfected cells (according to manufacturer's technical information). This antibody produce the same pattern of staining as the rabbit anti GPR151 polyclonal and is discussed below.
3. Rabbit VGLUT1 polyclonal antibody (135 303, Synaptic Systems) is generated against Strep-Tag® fusion protein of rat VGLUT1, containing amino acid residues 456–560 (*TLSGMVCPIIVGAMT)*. The antibody is affinity purified using the immunogen. Immunoreactivity in brain sections was abolished by pre-adsorption with the immunogen (Zhou et al., 2007). Western blot of lysate of cerebellum and cochlear nucleus in guinea pig detects a band at ~60 kDa. The molecular weight corresponds to what has previously been reported for the VGLUT1 protein (Takamori et al., 2000). No staining was observed in VGLUT1$^{-/-}$ mice (Wojcik et al., 2004).
4. Guinea pig VGLUT1 polyclonal antibody (135 304, Synaptic Systems) is generated against a purified recombinant protein of rat VGLUT 1, containing amino acid residues 456–560 (*TLSGMVCPIIVGAMT)*. The antibody recognizes one major broad band of the expected molecular weight (50–60 kDa) on western blots of a synaptic vesicle fraction of rat brain (LP2) and immunostaining is absent in VGLUT1$^{-/-}$ mice (according to the manufacturer). The antibody has been shown to produce an identical immunostaining pattern as the rabbit VGLUT1 polyclonal antibody in rat striatum and cortex (Wouterlood et al., 2012).

5. Rabbit VGLUT2 polyclonal antibody (135 403, Synaptic Systems) is raised against Strep-Tag® fusion protein of rat VGLUT2, containing amino acid residues 510–582 (*EKQPWADPEETSEEKCGFIHEDELDEETGDITQNYINYGTTKSYGATSQENGG WPNGEKKEEFVQESAQDAYSYKDRDDYS)*. Selective immunoreactivity in brain sections has been demonstrated by pre-adsorption with the immunogen (Zhou et al., 2007). Western blot of lysate of cerebellum and cochlear nucleus detects a band at ~65 kDa which corresponds to previous reports (Takamori et al., 2001).

6. Guinea pig VGLUT2 polyclonal antibody (135 404, Synaptic Systems) is generated against a purified recombinant protein of rat VGLUT2, containing amino acid residues 510–582 (*EKQPWADPEETSEEKCGFIHEDELDEETGDITQNYINYGTTKSYGATSQENGG WPNGEKKEEFVQESAQDAYSYKDRDDYS)*. The antibody recognizes one major broad band of the expected molecular weight (65 kDa) on western blots of a synaptic vesicle fraction of rat brain and immunostaining was abolished by pre-adsorption with the immunogen (according to the manufacturer). No cross-reactivity against VGLUT1 or VGLUT3 was observed.

7. Goat choline acetyltransferase (ChAT) polyclonal antibody (AB144P, Millipore) is raised against human placental choline acetyltransferase enzyme. The antibody recognizes a single band of 68–70 kDa on western blots of mouse brain (according to the manufacturer). This antibody has previously been used to investigate the expression of ChAT in the rat habenula (Aizawa et al., 2012) and yields the same pattern of expression as other ChAT antibodies (Contestabile et al., 1987).

8. Mouse neurofilament H monoclonal antibody (SMI-32R, clone SMI-32, Covance) is raised against homogenized hypothalami from Fischer 344 rat brain (Sternberger et al., 1982). This antibody recognizes a non-phosphorylated epitope on the neurofilament heavy polypeptide in human and monkey brain lysate (Campbell and Morrison, 1989). The antibody has previously been used to differentiate between different subnuclei in the rat and mouse LHb (Geisler et al., 2003; Wagner et al., 2014).

9. Mouse monoclonal tyrosine hydroxylase (TH) antibody (T1299, clone TH-2, Sigma-Aldrich) is derived from a hybridoma produced by the fusion of mouse myeloma cells and splenocytes from a mouse immunized against whole-rat TH protein (Haycock et al., 1993). The antibody recognizes an epitope (amino acids 9–16) present in the N-terminal region of both rodent (~60 kDa) and human (62–68 kDa) TH (Haycock et al., 1993). Its specificity for dopaminergic neurons was demonstrated by the topographic distribution of immunoreactive TH cell bodies and axon terminals in different brain regions and by their near total disappearance from mesencephalon and striatum after neonatal 6-OHDA lesion (Bérubé-Carrière et al., 2009).

10. Mouse tryptophan hydroxylase (TPH) monoclonal antibody (T0678, clone WH-3, Sigma-Aldrich) is raised against recombinant rabbit TPH. The antibody detects a band at 55 kDa on western blot of rabbit pineal gland (according to the

manufacturer). The pattern of immunoreactive cells marked by this antibody corresponded well to known serotonergic nuclei and has been used extensively as a marker of serotonergic neurons (Liu and Wong-Riley, 2010; Sevigny et al., 2012).

11. Sheep TPH polyclonal antibody (AB1541, Chemicon) is raised against a recombinant rabbit TPH, isolated as inclusion bodies from E. coli and purified by preparative SDS-PAGE. It recognizes a major band of 55 kDa molecular weight on western blot from rat dorsal raphe that corresponds to TPH; a less intense band can be observed at 62–65 kDa, indicating a partial cross-reactivity with TH (Chemicon datasheet). The cross-reactivity with TH did not affect our conclusions since we used the antibody only to localize the TPH-positive cell bodies present in the raphe nuclei. The antibody produces an identical pattern of staining as the mouse TPH monoclonal antibody and has previously been used to identify TPH expressing neurons in the raphe nuclei (Kaufling et al., 2009).

12. Rabbit substance P polyclonal antibody (20064, Immunostar) is raised against synthetic substance P coupled to keyhole limpet hemocyanin with carbodiimide. Immunolabeling was significant in rat dorsal horn and substantia nigra (according to the manufacturer). Pre-adsorption with substance P (10μg/ml) completely abolishes immunolabeling while incubation with neurokinin A, neurokinin B, somatostatin or neuropeptide K did not affect immunolabeling (manufacturer's specification; Weissner et al., 2006).

13. Rat substance P monoclonal antibody (sc-21715, Santa Cruz) is raised against eight-amino acids of the COOH-terminal fragment of substance P (NC1/34HL). The antibody does not cross react with β-endorphin, somatostatin, leu-enkephalin, or met-enkephalin. The specificity was verified by pre-adsorption with synthetic substance P (220μg/ml) (Cuello et al., 1979).

14. Chicken β-galactosidase polyclonal antibody (AB9361, Abcam) is raised against the purified full length native Escherichia coli (E. coli) protein and immunoaffinity purified using purified β-galactosidase immobilized on a solid phase. The antibody specificity was confirmed by the absence of staining in wild-type animals.

RESULTS

Comparable expression of GPR151 in habenular axonal projections in rat and mouse brain

To begin to assess the expression pattern of GPR151 we analyzed serial brain section of mouse and rat using two different antibodies against GPR151. Both antibodies yielded robust and comparable immunoreactivity in habenular axons, and no signal was detected in brain sections of *Gpr151*$^{-/-}$ mice (Fig. 1 A1–J1) confirming the antibody specificity. GPR151 immunoreactivity was detected in axonal fibers originating in the habenula (Fig. 1 A,B), continuing through the fasciculus retroflexus (FR) (Fig. 1 C,D) and contacting the IPN (Fig. 1 E,F). Caudal to the IPN, GPR151 immunoreactive fibers continued in a dorsocaudal direction through the RMTg (Fig. 1 F,G), rhabdoid nucleus (Fig. 1 G,H), median and paramedian raphe (Fig. 1G,H) and dorsal raphe nucleus (Fig. 1 I,J). Comparative analyses of mouse and rat brains at similar section planes revealed a strikingly high similarity in the

pattern of GPR151-immunoreactive neuronal projections between mouse (Fig. 1 A–J) and rat (Fig. 1 A2–J2)

Conserved GPR151 immunoreactivity in the habenular circuitry of zebrafish

Interestingly the human *GPR151* gene shows 54% identity with two loci in the zebrafish genome that may encode two probable Gpr151-like receptors, which only differ between each other in one amino acid residue (NCBI HomoloGene). These two loci LOC100538082 and LOC565170 are in very close proximity to each other in chromosome 14 of *D. rerio* adjacent to two genes (tcerg1 and ppp2r2), which are also neighboring *GPR151* in chromosome 5 in the human genome. This raises the possibility that the genomic locus containing *GPR151* has been preserved during evolution but that one copy of the probable *Gpr151-like* receptor gene in zebrafish has been lost in higher vertebrates.

We wanted to test whether antibodies raised against the human GPR151 protein could recognize the zebrafish putative Gpr151-like receptor, which shows 45% identity at the protein level. As shown in figure 2, a remarkably similar and selective immunoreactivity for habenular circuitry as found in rat and mouse brain was also seen in the zebrafish with strong expression in axonal projections originating in the habenula (Fig. 2A), and coursing via the FR (Fig. 2B) to the IPN (Fig. 2C) and ventral median raphe (Fig. 2D). Double immunofluorescence staining using rabbit and mouse polyclonal antibodies resulted in completely overlapping labeling (data not shown). Tracing and immunostaining studies in zebrafish have determined that the dorsal habenula is asymmetric, projects to the IPN and corresponds to the MHb of mammals, while the ventral habenula is homologous to the LHb in mammals, projects to the median raphe and is not lateralized (Amo et al., 2010). Thus, consistent with GPR151 expression in MHb and LHb projections in rodents, Gpr151 is present in the homologous habenular axonal projections to the IPN and raphe in zebrafish. Dense immunoreactivity was observed in fibers in the dorsal habenula while the ventral habenula was only very sparsely labeled. This pattern was also reflected in the strong Gpr151 positive innervation of the interpeduncular nucleus, while only a few axon terminals were observed in the ventral median raphe (Fig. 2). Altogether, these results show that the protein expression pattern of GPR151 is highly conserved.

Expression of GPR151 in habenular subnuclei

We next examined in detail the expression of GPR151 in the habenula. To this end we compared the GPR151 immunoreactivity to the *lacZ* reporter signal in *Gpr151*$^{-/-}$ mice (Fig. 3A) and to different markers that have been employed to subdivide the habenular subnuclei in mouse and rat (Fig. 3B–U). The MHb can be subdivided in a ventral (vMHb) and a dorsal (dMHb) part. Neurons in the dMHb express substance P (SP) (Contestabile et al., 1987; Cuello et al., 1978) and project to the rostral and lateral subnuclei of the IPN (Contestabile et al., 1987). Neurons in the vMHb express the ACh synthesizing enzyme choline acetyltransferase (ChAT) (Aizawa et al., 2012) and project to the central and intermediate subnuclei of IPN (Contestabile et al., 1987). In the MHb, GPR151 was detected in the cholinergic vMHb (Fig. 3C–E, M–O), but not in the SP expressing dMHb (Fig. 3B, F–H, P–R). In *Gpr151*$^{-/-}$ mice, where the bacterial *lacZ* reporter gene is expressed under the control of the *Gpr151* gene regulatory sequences, βGal immunoreactivity was confined to habenular

cell bodies (Fig. 3A). In the MHb βGal-positive cells were only detected in vMHb, consistent with in situ hybridization reports for *Gpr151* mRNA (Aizawa et al., 2012).

In addition GPR151 was also present in the LHb. To evaluate the localization of GPR151 within subnuclei of the LHb, we used the delineation of habenular subdivisions in rat and mouse proposed by Wagner and colleagues (Wagner et al., 2014). The LHb is composed of a medial and a lateral subregion. The medial LHb is further subdivided into the superior (LHbMS), parvocellular (LHbMPc), central (LHbMC), marginal (LHbMMg) subnuclei (Fig. 3A,B,L). The lateral LHb is subdivided into the parvocellular (LHbLPc), magnocellular (LHbLMc), oval (LHbLO), basal (LHbLB), and marginal (LHbLMg) subnuclei (Fig. 3A,B,L). Consistent with the previously reported expression of *Gpr151* mRNA (Aizawa et al., 2012), βGal-positive cells in *Gpr151*$^{-/-}$ mice were scattered throughout the LHb with a tendency for a more marked expression in the dorsal part (containing the LHbMS and LHbLPc) (Fig. 3A). In addition, given that neurofilament H (NF-H) has been used as a marker to delineate the LHb subnuclei of rat and mouse brain sections (Geisler et al., 2003; Wagner et al., 2014), we performed colabeling of GPR151 and NF-H. As observed in figure 3, LHbMPc and LHbMC are completely devoid of NF-H immunoreactivity. In contrast, GPR151 immunoreactivity is strongly expressed in these subnuclei (Fig. 3I–K, L, S–U).

GPR151 expression in habenular efferents projecting to the IPN and not the VTA

Given that Gpr151 mRNA and βGal reporter expression is highly concentrated in the MHb (Fig 3A; Görlich et al., 2013) and that the major output of the MHb is the IPN, we next investigated the expression of GPR151 in habenular axons that innervate the IPN. GPR151 expression was extremely prominent in the rostral (IPR), dorsomedial (IPDM), dorsolateral (IPDL) and apical subnuclei (IPA) but immunoreactivity in the central (IPC), intermediate (IPI) and lateral IPN (IPL) was also observed (Fig. 4,5,6). It has been shown that the vesicular glutamate transporter VGLUT1 is expressed in MHb neurons but not in LHb neurons (Aizawa et al., 2012) and that within the MHb, cholinergic neurons in the ventral part co-release ACh and glutamate (Ren et al., 2011). Therefore we performed double staining of GPR151 with ChAT (Fig. 4A–H) and VGLUT1 (Fig. 4I–P) antibodies to evaluate whether GPR151 is specifically expressed in cholinergic and/or glutamatergic terminals. In order to quantify the degree of overlap we calculated Manders' colocalization coefficient. The statistical significance of this colocalization was given by the Costes' P-value. Colocalization between GPR151 and VGLUT1 was statistically significant (mouse, P=1.0; rat, P=1.0) and moderately overlapping (Fig. 4I–P; mouse M1=0.71; rat M1=0.88). A significant and more pronounced colocalization of GPR151 and ChAT was observed in the rostral subnucleus and in the dorsal part of the central subnucleus (Fig. 4A–H; mouse M1=0.83, P=1.0; rat M1=0.99, P=1.0). These results indicate that a major proportion of GPR151 habenular fibers projecting to the IPN are glutamatergic and that a high number are cholinergic. Possibly, those GPR151-fibers are both glutamatergic and cholinergic (Ren et al., 2011).

The VTA is adjacent to the IPN and innervated by LHb (Herkenham and Nauta, 1979). To evaluate whether GPR151 positive axonal fibers innervate this region, we performed

immunostaining for the dopaminergic marker tyrosine hydroxylase (TH). This marker delineates the sharp boundary between the IPN and the VTA (Fig. 5B,E). Colabeling with GPR151 and TH in mouse and rat brain section clearly show that LHb neurons that express GPR151 do not terminate in the VTA region (Fig. 5A–F).

GPR151 expression in habenular neurons projecting to the RMTg and rhabdoid nucleus

In addition to the VTA, the LHb has been shown to project to forebrain areas including the ventrolateral septum and the substantia innominata, to midbrain areas including the RMTg, to the median and dorsal raphe nuclei and to hindbrain areas, including the laterodorsal and dorsal tegmental nucleus, the locus coeruleus (Herkenham and Nauta, 1979; Jhou et al., 2009b; Lecourtier and Kelly, 2007) and the nucleus incertus (Goto et al., 2001; Olucha-Bordonau et al., 2003). We analyzed sagittal sections including forebrain, midbrain and hindbrain regions and detected habenular GPR151 fibers continuing caudally through the IPN, via the rhabdoid nucleus reaching mesencephalic raphe nuclei and the dorsal tegmental nucleus (Fig. 6). However, no immunoreactivity was observed in the forebrain, indicating that GPR151 positive neurons of the habenula do not project to forebrain areas. The rhabdoid nucleus is a bilateral structure extending from the IPN to the dorsal raphe nucleus and the dorsal tegmentum (Fig. 6). To examine whether GPR151 immunoreactive projections in the rhabdoid nucleus originated from glutamatergic LHb neurons, we performed double immunolabeling of GPR151 and VGLUT2 (Fig. 7A–J). A statistically significant colocalization of GPR151 and VGLUT2 was observed in the rhabdoid nucleus (Fig. 7A–J; mouse M1=0.82, P=1.0; rat M1=0.59, P=1.0). This finding supports that at least part of the GPR151 positive neurons may be glutamatergic. Since previous studies have demonstrated dense SP immunoreactivity in the rhabdoid nucleus (Paxinos, 2004), we next carried out GPR151 and SP double immunofluorescence stainings. Even though partial colocalization of SP and GPR151 in the rhabdoid nucleus was revealed (Fig. 7K–T; mouse M1=0.65, P=1.0; rat M1=0.84, P=1.0), we cannot conclude whether GPR151 projections from the LHb are also SP-ergic or whether GPR151 projections from LHb are travelling together with SP fibers originating elsewhere.

Furthermore, the LHb has been shown to send glutamatergic projections to the RMTg which acts as an inhibitory center of the midbrain dopaminergic cells (Balcita-Pedicino et al., 2011; Ferreira et al., 2008; Geisler and Zahm, 2005; Jhou et al., 2009a). The RMTg, also known as the tail of the VTA, extends from the caudal pole of the VTA into the mesopontine tegmentum (Jhou et al., 2009a,b; Bourdy and Barrot, 2012). GPR151 immunofluorescence staining on mouse and rat coronal sections showed heavy GPR151 expression in RMTg (Fig. 8). Since most LHb neurons are glutamatergic and known to express the vesicular glutamate transporter 2 (VGLUT2) (Aizawa et al., 2012), we performed double labeling for this transporter and GPR151. Colocalization was indeed observed in terminals located in the RMTg (Fig. 8; mouse M1=0.72, P=1.0; rat M1=0.62, P=1.0), indicating the existence of glutamatergic GPR151 positive neurons projecting from the LHb to the RMTg.

GPR151 immunoreactive projections to the mesencephalic raphe nuclei and the dorsal tegmental nucleus

We next analyzed GPR151 immunoreactive projections to the mesencephalic raphe nuclei. Results from previous anterograde tracing studies targeting the LHb show labeling at the median, paramedian and dorsal raphe nucleus (Gonçalves et al., 2012; Kim, 2009; Sego et al., 2014). In agreement with these studies, we observed GPR151 positive fibers (presumably originating in the LHb) in the median, paramedian and dorsal raphe (Fig. 6 and 9).

GPR151 immunostaining in coronal rat and mouse brain sections at the level of the dorsal raphe showed GPR151 expression particularly in the interfascicular and caudal subnucleus (Fig. 9). Some GPR151 positive fibers appear to make contact with serotonergic neurons positive for the tryptophan hydroxylase (TPH) serotonergic marker (Fig. 9D–F,J–L, arrows), suggesting that LHb GPR151 expressing neurons may be implicated in dorsal raphe functions such as motivation and reward seeking.

In addition to GPR151 expression in the dorsal raphe, we also observed sparse GPR151 immunoreactivity in the dorsal tegmental nucleus in both sagittal (Fig. 6) and coronal rodent brain sections (Fig. 9A–C,G–I). Projections from LHb to the dorsal tegmental nucleus have been previously documented (Liu et al., 1984; Kim, 2009).

DISCUSSION

In the present study we investigated the anatomical and subcellular protein localization of the G protein-coupled receptor GPR151 in the brain of mammals and fish. We show that this receptor marks a specific and conserved subset of habenular axonal projections in vertebrates. GPR151 is not expressed in the soma of habenular neurons, but in their axonal projections. GPR151 immunoreactivity in selective habenular axonal projections and colocalization with neurotransmitter marker proteins, establish that GPR151 positive neurons in habenula project to the IPN, the RMTg, the rhabdoid nucleus, the mesencephalic raphe nuclei and the dorsal tegmentum (Fig. 10). Below we discuss the conservation of habenular nuclei in mouse and rat evidenced by GPR151 topographic distribution, and the specific axonal projections to discrete nuclei in the midbrain.

GPR151 immunoreactivity highlights the conservation of habenula subnuclear architecture

In the present study, we investigated the expression of GPR151 by immunohistochemical analysis of rat and mouse brain sections and confirmed the specificity of the antibodies using *Gpr151*$^{-/-}$ mice. Consistent with *Gpr151* mRNA expression (Aizawa et al., 2012) we observed immuno βGal staining in *Gpr151*$^{-/-}$ mice containing the lacZ reporter in the ventral MHb and scattered throughout the LHb with a marked expression in LHbMS (Fig. 3A).

We found that GPR151 immunoreactivity is not localized to neuronal cell bodies, but to their axonal projections. Within the habenula, GPR151 positive neurites are especially enriched in the parvocellular subnucleus LHbMPc (Fig. 3), a subnucleus in the LHb reliably

detected because it is largely devoid of neurofilament-H (NF-H) both in rat and mouse. Nissl staining of this area shows densely packed small neurons in agreement with its designation as the parvocellular subnucleus (Wagner et al., 2014). Interestingly this subnucleus has very weak *Gpr151* in situ hybridization signal (Aizawa et al., 2012) and lacks βGal immunoreactivity in *Gpr151*$^{-/-}$ mice (Fig. 3A), indicating that cell bodies in the LHbMPc do not express the GPR151 protein. However, it is remarkable that LHbMPc is transversed by very few fibers positive for NF-H and Kir2.3 which both label dense fiber complexes in other habenula subnuclei (Geisler et al., 2003; Wagner et al., 2014). Kir2.3 channel subunits are expressed in dendrites in many types of neurons (Inanobe et al., 2002), while NF-H is abundant in large dendritic trees (Kong et al., 1998) but also expressed in axons (Marszalek et al., 1996). Given the dense network of GPR151-positive fibers in the LHbMPc, and the lack of Kir2.3 and NF-H in this subnucleus, it is tempting to speculate that these fibers are indeed habenular axons converging at this site and continuing through the FR to target areas in the brainstem. Although topographically organized commissural projections from the LHb to the contralateral LHb have been described (Kim, 2009), these do not seem to project to the LHbMPc but to more central and lateral LHb subnuclei. In conclusion, GPR151 is a valuable marker to identify and correlate several subnuclei in rat and mice habenula including the cholinergic ventral medial habenula and the conspicuous LHbMPc.

Habenular GPR151 positive projections to the IPN

While it is established that the major input to the IPN originates in the MHb and that these projections are organized in a dorso-ventral to latero-central topographic manner (i.e. substance P projections from the dorsal MHb to the IPL and cholinergic projections from the ventral MHb to the IPC), it has been controversial and much more difficult to visualize whether the lateral habenula also sends projections to the IPN (Kim, 2009). In the present study we detected very intense GPR151 immunoreactivity in habenular axons terminating in the IPN. In the IPC, GPR151 immunoreactivity colocalized with ChAT and the glutamatergic marker VGLUT1 (Fig. 4). This is consistent with the fact that GPR151 is highly enriched in cholinergic neurons located in the ventral medial habenula (Görlich et al., 2013; Aizawa et al., 2012; Fig. 3) that project mainly to the IPC and co-release glutamate (Ren et al., 2011). However GPR151 was also present in non-cholinergic habenular terminals in the IPL (Fig. 4A,E), which is mostly innervated by substance P projections form the dorsal MHb. Since GPR151 is not expressed in the dorsal MHb (Fig. 3), these results indicate that the GPR151 positive projections that we detect in the IPL might in fact originate from the lateral habenula. Such projections to the IPL have been visualized using anterograde tracers injected in the central and medial subregions of the lateral habenula (Kim, 2009).

This is interesting as it indicates that GPR151-positive projections from both the lateral and medial habenula terminate in the IPN. Given that the cholinergic MHb-IPN circuit has emerged as key pathway in the regulation of nicotine reinforcement, dependence and withdrawal (Fowler et al., 2011; Frahm et al., 2011; Glick et al., 2011; Salas et al., 2009), it is tempting to hypothesize that GPR151 modulates nicotine-mediated behaviors.

Habenular GPR151 positive projections to the RMTg

The LHb has been shown to project predominantly to the substantia nigra, VTA, raphe nuclei (Herkenham and Nauta, 1979) and RMTg (Gonçalves et al., 2012; Jhou et al., 2009b; Kaufling et al., 2009). Interestingly we did not observe GPR151 staining in the substantia nigra or in the VTA (Fig. 5), indicating that GPR151 is not expressed in the subpopulation of LHb neurons that directly innervate these dopaminergic areas. However we detected strong immunoreactivity in the RMTg (Fig. 8) and since the RMTg acts as an inhibitory center of the substantia nigra and VTA (Balcita-Pedicino et al., 2011; Ferreira et al., 2008; Geisler and Zahm, 2005; Jhou et al., 2009a), it is possible that GPR151 positive habenular efferents to the RMTg indirectly modulate dopaminergic neurons in the midbrain, and thereby the motivational aspects of reinforcement learning and decision-making. In fact, specific (diphtheria toxin-mediated) ablation of neurons expressing *Gpr151* caused a broad range of cognitive deficits, including delay and effort aversion in a decision-making test (Kobayashi et al., 2013). RMTg neurons also project to the dorsal raphe where they terminate mainly on glutamatergic neurons (Lavezzi et al., 2011; Sego et al., 2014). Further studies are needed to determine if the neurons in the RMTg innervated by GPR151 habenular axons, preferentially target VTA, substantia nigra or the dorsal raphe.

Habenular GPR151 positive projections to the rhabdoid nucleus

In addition we observed strong GPR151 immunolabeling in the rhabdoid nucleus (Figure 6–8). The rhabdoid nucleus is a bilateral structure dorsal to the median raphe nucleus that stretches from the IPN to the dorsal raphe nucleus (Fig. 6), and is readily visible in acetylcholine esterase histochemical preparations (Paxinos and Watson, 2006). The nucleus has previously been reported to exhibit rich substance P immunoreactivity (Paxinos, 2004), which was confirmed in our study (Fig. 7). Projections from habenula to the rhabdoid nucleus have not previously been described. In fact, the connectivity and function of the rhabdoid nucleus is poorly understood. One study showed substance P containing axons that appeared to originate from the dorsal rhabdoid nucleus and terminate primarily on dendrites of serotonergic neurons (Lacoste et al., 2009). Bilateral lesioning of the habenula abolished substance P immunoreactivity in this region. Habenular lesions also decreased the concentration of substance P in the dorsal raphe (Neckers et al., 1979; Vincent et al., 1980). Given that substance P has been reported to have both excitatory and inhibitory effects on neurons in the dorsal raphe (Valentino et al., 2003), and that these terminals coexpress GPR151, it could be hypothesized that GPR151 regulates substance P neurotransmission in the dorsal raphe and thereby modulating serotonergic neuronal activity. The origin of the substance P in the rhabdoid nucleus, is not clear. We detected substance P neurons in the dorsal MHb, but this region is devoid of *Gpr151* expressing neurons (Fig. 3A; Aizawa et al., 2012). However, we also observed substance P immunoreactivity in neurons of the medial part of the LHb which show scattered expression of *Gpr151* (Fig. 3A). Further studies at electronmicroscopic level are needed to clarify the details of substance P and GPR151 expression in the rhabdoid nucleus. Nonetheless the studies presented here demonstrate that GPR151 can be used as a marker to localize the rhabdoid nucleus, which could facilitate further studies to gain insight into the biological role of this brain area.

GPR151 habenular projections to brainstem serotonergic nuclei

We also detected GPR151 positive fibers in the serotonergic median, paramedian and dorsal raphe nuclei (Fig. 9). Both indirect and direct habenular projections to serotonergic neurons in the dorsal raphe have previously been reported. In the present study, we observed GPR151 positive fibers making contact to serotonergic neurons in the dorsal raphe (Fig. 9, arrows). Electrical stimulation of the LHb decreases serotonin release in the caudate nucleus and substantia nigra, an effect that could be blocked by infusion of the $GABA_A$ receptor antagonist picrotoxin in the dorsal raphe (Reisine et al., 1982). Stimulation of the LHb also modulates serotonin release in the hippocampus, mediated through both direct and indirect projections to the dorsal raphe (Ferraro et al., 1997). The presence of GPR151 in axonal terminals innervating serotonergic neurons, raises the possibility that GPR151 could modulate serotonin release, which in turn would have implications for pain, stress, sleep and depressive-like behavior.

GPR151 habenular projections to the dorsal tegmental nucleus

Finally, we observed GPR151 immunoreactive axons projecting to the dorsal tegmental nucleus, mainly to the central part (DTgC) (Fig. 6 and 9). This is in agreement with previous reports describing the projections from LHb to the dorsal tegmental nucleus (Liu et al., 1984). The dorsal tegmental nucleus contains cells that signal the animal's momentary directional heading and thus it is thought to be involved in navigation. Moreover, Sharp et al. reported that activity of 10% of the LHb neurons correlated with angular head motion (Sharp et al., 2006). In summary, GPR151 may possibly modulate these functions controlled by the dorsal tegmental nucleus.

CONCLUDING REMARKS

In summary, GPR151 expression in the rat, mouse and zebrafish brain is restricted to habenular neurons projecting to the IPN, RMTg, rhabdoid nucleus, mesencephalic raphe nuclei and dorsal tegmental nucleus. The medial and lateral habenula have traditionally been considered as functionally segregated. However GPR151 expression in both habenular subdivisions raises the possibility that GPR151 projection targets may constitute a functional system. Through modulation of cholinergic, serotonergic and peptidergic neuronal circuits in the brainstem, GPR151 may coordinate functions related to addiction, reinforcement learning, decision-making, pain processing and depression. For instance, can addiction be considered an impairment in decision-making, or is withdrawal a form of unexpected negative reward, and how can these behaviors relate to pain processing and depression? Altogether, the fact that GPR151 is highly conserved from lower vertebrates to mammals, including humans (Hawrylycz et al., 2012), and that it belongs to the highly druggable Class A of GPCRs, makes it a potential target for novel treatment modalities for common and devastating psychiatric maladies such as mood disorders and drug dependence.

Acknowledgments

This work was supported by the Bror Gadelius memorial fund (JB and AT) and the NIH/NIDA grant 1P30 DA035756-01 (BAF and IIT).

The authors thank Madeleine Åberg Andersson, Fredrik Ek and Sylvia Lipford for their technical assistance. This work was supported by the NIH/NIDA grant 1P30 DA035756-01 (II-T), and a grant from the Bror Gadelius memorial fund.

Glossary

3V	Third ventricle
4V	Fourth ventricle
CLi	Central linear nucleus of the raphe
dIPN	Dorsal part of the interpeduncular nucleus
dMHb	Dorsal part of the medial habenula
DRC	Caudal part of the dorsal raphe
DRD	Dorsal part of the dorsal raphe
DRI	Interfascicular part of the dorsal raphe
DRV	Ventral part of the dorsal raphe
DTg	Dorsal tegmental nucleus
DTgC	Central part of the dorsal tegmental nucleus
DTgP	Pericent part of the dorsal tegmental nucleus
FR	Fasciculus retroflexus
IPA	Apical part of the interpeduncular nucleus
IPC	Central part of the interpeduncular nucleus
IPDL	Dorsolateral part of the interpeduncular nucleus
IPDM	Dorsomedial part of the interpeduncular nucleus
IPI	Intermediate part of the interpeduncular nucleus
IPL	Lateral part of the interpeduncular nucleus
IPN	Interpeduncular nucleus
IPR	Rostral part of the interpeduncular nucleus
IPRL	Rostrolateral part of the interpeduncular nucleus
LDTg	Laterodorsal tegmental nucleus
LHb	Lateral habenula
LHbLB	Basal subnucleus of the lateral part of the LHb
LHbLMc	Magnocellular subnucleus of the lateral part of the LHb
LHbLMg	Marginal subnucleus of the lateral part of the LHb
LHbLO	Oval subnucleus of the lateral part of the LHb
LHbLPc	Parvocellular subnucleus of the lateral part of the LHb

LHbMC	Central subnucleus of the medial part of the LHb
LHbMMg	Marginal subnucleus of the medial part of the LHb
LHbMPc	Parvocellular subnucleus of the medial part of the LHb
LHbMS	Superior subnucleus of the medial part of the LHb
MHb	Medial habenula
mlf	Medial longitudinal fasciculus
MnR	Median raphe nucleus
PDTg	Posterodorsal tegmental nucleus
PMnR	Paramedian raphe nucleus
Rbd	Rhabdoid nucleus
RMTg	Rostromedial tegmental nucleus
scp	Superior cerebellar peduncle
vIPN	Ventral part of the interpeduncular nucleus
vMHb	Ventral part of the medial habenula
VTA	Ventral tegmental area

LITERATURE CITED

Aizawa H, Kobayashi M, Tanaka S, Fukai T, Okamoto H. Molecular characterization of the subnuclei in rat habenula. J Comp Neurol. 2012; 520:4051–4066. [PubMed: 22700183]

Amo R, Aizawa H, Takahoko M, Kobayashi M, Takahashi R, Aoki T, Okamoto H. Identification of the zebrafish ventral habenula as a homolog of the mammalian lateral habenula. J Neurosci. 2010; 30:1566–1574. [PubMed: 20107084]

Andres KH, von Düring M, Veh RW. Subnuclear organization of the rat habenular complexes. J Comp Neurol. 1999; 407:130–150. [PubMed: 10213193]

Balcita-Pedicino JJ, Omelchenko N, Bell R, Sesack SR. The inhibitory influence of the lateral habenula on midbrain dopamine cells: Ultrastructural evidence for indirect mediation via the rostromedial mesopontine tegmental nucleus. J Comp Neurol. 2011; 519:1143–1164. [PubMed: 21344406]

Berrettini W, Yuan X, Tozzi F, Song K, Francks C, Chilcoat H, Waterworth D, Muglia P, Mooser V. Alpha-5/alpha-3 nicotinic receptor subunit alleles increase risk for heavy smoking. Mol Psychiatry. 2008; 13:368–373. [PubMed: 18227835]

Berthold M, Collin M, Sejlitz T, Meister B, Lind P. Cloning of a novel orphan G protein-coupled receptor (GPCR-2037): in situ hybridization reveals high mRNA expression in rat brain restricted to neurons of the habenular complex. Brain Res Mol Brain Res. 2003; 120:22–29. [PubMed: 14667573]

Bérubé-Carrière N, Riad M, Dal Bo G, Lévesque D, Trudeau L-E, Descarries L. The dual dopamine-glutamate phenotype of growing mesencephalic neurons regresses in mature rat brain. J Comp Neurol. 2009; 517:873–891. [PubMed: 19844994]

Bérubé-Carrière N, Guay G, Fortin GM, Kullander K, Olson L, Wallén-Mackenzie Å, Trudeau L-E, Descarries L. Ultrastructural characterization of the mesostriatal dopamine innervation in mice, including two mouse lines of conditional VGLUT2 knockout in dopamine neurons. Eur J Neurosci. 2012; 35:527–538. [PubMed: 22330100]

Bianco IH, Wilson SW. The habenular nuclei: a conserved asymmetric relay station in the vertebrate brain. Philos Trans R Soc Lond, B, Biol Sci. 2009; 364:1005–1020. [PubMed: 19064356]

Bierut LJ, Stitzel JA, Wang JC, Hinrichs AL, Grucza RA, Xuei X, Saccone NL, Saccone SF, Bertelsen S, Fox L, Horton WJ, Breslau N, Budde J, Cloninger CR, Dick DM, Foroud T, Hatsukami D, Hesselbrock V, Johnson EO, Kramer J, Kuperman S, Madden PAF, Mayo K, Nurnberger J, Pomerleau O, Porjesz B, Reyes O, Schuckit M, Swan G, Tischfield JA, Edenberg HJ, Rice JP, Goate AM. Variants in nicotinic receptors and risk for nicotine dependence. Am J Psychiatry. 2008; 165:1163–1171. [PubMed: 18519524]

Bromberg-Martin ES, Matsumoto M, Hikosaka O. Distinct tonic and phasic anticipatory activity in lateral habenula and dopamine neurons. Neuron. 2010; 67:144–155. [PubMed: 20624598]

Caldecott-Hazard S, Mazziotta J, Phelps M. Cerebral correlates of depressed behavior in rats, visualized using 14C-2-deoxyglucose autoradiography. J Neurosci. 1988; 8:1951–1961. [PubMed: 3385484]

Campbell MJ, Morrison JH. Monoclonal antibody to neurofilament protein (SMI-32) labels a subpopulation of pyramidal neurons in the human and monkey neocortex. J Comp Neurol. 1989; 282:191–205. [PubMed: 2496154]

Contestabile A, Villani L, Fasolo A, Franzoni MF, Gribaudo L, Oktedalen O, Fonnum F. Topography of cholinergic and substance P pathways in the habenulo-interpeduncular system of the rat. An immunocytochemical and microchemical approach. Neuroscience. 1987; 21:253–270. [PubMed: 2439945]

Costes SV, Daelemans D, Cho EH, Dobbin Z, Pavlakis G, Lockett S. Automatic and quantitative measurement of protein-protein colocalization in live cells. Biophys J. 2004; 86:3993–4003. [PubMed: 15189895]

Cuello AC, Emson PC, Paxinos G, Jessell T. Substance P containing and cholinergic projections from the habenula. Brain Res. 1978; 149:413–429. [PubMed: 352479]

Cuello AC, Galfre G, Milstein C. Detection of substance P in the central nervous system by a monoclonal antibody. Proc Natl Acad Sci USA. 1979; 76:3532–3536. [PubMed: 386341]

Dunn KW, Kamocka MM, McDonald JH. A practical guide to evaluating colocalization in biological microscopy. Am J Physiol, Cell Physiol. 2011; 300:C723–42. [PubMed: 21209361]

Ferraro G, Montalbano ME, Sardo P, La Grutta V. Lateral habenula and hippocampus: a complex interaction raphe cells-mediated. Journal of neural transmission (Vienna, Austria: 1996). 1997; 104:615–631.

Ferreira JGP, Del-Fava F, Hasue RH, Shammah-Lagnado SJ. Organization of ventral tegmental area projections to the ventral tegmental area-nigral complex in the rat. Neuroscience. 2008; 153:196–213. [PubMed: 18358616]

Fowler CD, Lu Q, Johnson PM, Marks MJ, Kenny PJ. Habenular α5 nicotinic receptor subunit signalling controls nicotine intake. Nature. 2011; 471:597–601. [PubMed: 21278726]

Frahm S, Slimak MA, Ferrarese L, Santos-Torres J, Antolin-Fontes B, Auer S, Filkin S, Pons S, Fontaine J-F, Tsetlin V, Maskos U, Ibañez-Tallon I. Aversion to nicotine is regulated by the balanced activity of β4 and α5 nicotinic receptor subunits in the medial habenula. Neuron. 2011; 70:522–535. [PubMed: 21555077]

Geisler S, Andres KH, Veh RW. Morphologic and cytochemical criteria for the identification and delineation of individual subnuclei within the lateral habenular complex of the rat. J Comp Neurol. 2003; 458:78–97. [PubMed: 12577324]

Geisler S, Zahm DS. Afferents of the ventral tegmental area in the rat-anatomical substratum for integrative functions. J Comp Neurol. 2005; 490:270–294. [PubMed: 16082674]

Gonçalves L, Sego C, Metzger M. Differential projections from the lateral habenula to the rostromedial tegmental nucleus and ventral tegmental area in the rat. J Comp Neurol. 2012; 520:1278–1300. [PubMed: 22020635]

Goto M, Swanson LW, Canteras NS. Connections of the nucleus incertus. J Comp Neurol. 2001; 438:86–122. [PubMed: 11503154]

Görlich A, Antolin-Fontes B, Ables JL, Frahm S, Slimak MA, Dougherty JD, Ibañez-Tallon I. Reexposure to nicotine during withdrawal increases the pacemaking activity of cholinergic habenular neurons. Proc Natl Acad Sci USA. 2013; 110:17077–17082. [PubMed: 24082085]

Hawrylycz MJ, Lein ES, Guillozet-Bongaarts AL, Shen EH, Ng L, Miller JA, van de Lagemaat LN, Smith KA, Ebbert A, Riley ZL, Abajian C, Beckmann CF, Bernard A, Bertagnolli D, Boe AF, Cartagena PM, Chakravarty MM, Chapin M, Chong J, Dalley RA, Daly BD, Dang C, Datta S, Dee N, Dolbeare TA, Faber V, Feng D, Fowler DR, Goldy J, Gregor BW, Haradon Z, Haynor DR, Hohmann JG, Horvath S, Howard RE, Jeromin A, Jochim JM, Kinnunen M, Lau C, Lazarz ET, Lee C, Lemon TA, Li L, Li Y, Morris JA, Overly CC, Parker PD, Parry SE, Reding M, Royall JJ, Schulkin J, Sequeira PA, Slaughterbeck CR, Smith SC, Sodt AJ, Sunkin SM, Swanson BE, Vawter MP, Williams D, Wohnoutka P, Zielke HR, Geschwind DH, Hof PR, Smith SM, Koch C, Grant SGN, Jones AR. An anatomically comprehensive atlas of the adult human brain transcriptome. Nature. 2012; 489:391–399. [PubMed: 22996553]

Haycock JW. Multiple forms of tyrosine hydroxylase in human neuroblastoma cells: quantitation with isoform-specific antibodies. J Neurochem. 1993; 60:493–502. [PubMed: 8093479]

Herkenham M, Nauta WJ. Afferent connections of the habenular nuclei in the rat. A horseradish peroxidase study, with a note on the fiber-of-passage problem. J Comp Neurol. 1977; 173:123–146. [PubMed: 845280]

Herkenham M, Nauta WJ. Efferent connections of the habenular nuclei in the rat. J Comp Neurol. 1979; 187:19–47. [PubMed: 226566]

Hikosaka O. The habenula: from stress evasion to value-based decision-making. Nat Rev Neurosci. 2010; 11:503–513. [PubMed: 20559337]

Hsu Y-WA, Tempest L, Quina LA, Wei AD, Zeng H, Turner EE. Medial habenula output circuit mediated by α5 nicotinic receptor-expressing GABAergic neurons in the interpeduncular nucleus. J Neurosci. 2013; 33:18022–18035. [PubMed: 24227714]

Ignatov A, Hermans-Borgmeyer I, Schaller HC. Cloning and characterization of a novel G-protein-coupled receptor with homology to galanin receptors. Neuropharmacology. 2004; 46:1114–1120. [PubMed: 15111018]

Inanobe A, Fujita A, Ito M, Tomoike H, Inageda K, Kurachi Y. Inward rectifier K+ channel Kir2.3 is localized at the postsynaptic membrane of excitatory synapses. Am J Physiol, Cell Physiol. 2002; 282:C1396–403. [PubMed: 11997254]

Jhou TC, Fields HL, Baxter MG, Saper CB, Holland PC. The rostromedial tegmental nucleus (RMTg), a GABAergic afferent to midbrain dopamine neurons, encodes aversive stimuli and inhibits motor responses. Neuron. 2009a; 61:786–800. [PubMed: 19285474]

Jhou TC, Geisler S, Marinelli M, Degarmo BA, Zahm DS. The mesopontine rostromedial tegmental nucleus: A structure targeted by the lateral habenula that projects to the ventral tegmental area of Tsai and substantia nigra compacta. J Comp Neurol. 2009b; 513:566–596. [PubMed: 19235216]

Kaufling J, Veinante P, Pawlowski SA, Freund-Mercier M-J, Barrot M. Afferents to the GABAergic tail of the ventral tegmental area in the rat. J Comp Neurol. 2009; 513:597–621. [PubMed: 19235223]

Kim U, Chang S-Y. Dendritic morphology, local circuitry, and intrinsic electrophysiology of neurons in the rat medial and lateral habenular nuclei of the epithalamus. J Comp Neurol. 2005; 483:236–250. [PubMed: 15678472]

Kim U. Topographic commissural and descending projections of the habenula in the rat. J Comp Neurol. 2009; 513:173–187. [PubMed: 19123238]

Kobayashi Y, Sano Y, Vannoni E, Goto H, Suzuki H, Oba A, Kawasaki H, Kanba S, Lipp HP, Murphy NP, Wolfer DP, Itohara S. Genetic dissection of medial habenula–interpeduncular nucleus pathway function in mice. Frontiers in Behavioral Neuroscience. 2013; 7:17. [PubMed: 23487260]

Kong J, Tung VW, Aghajanian J, Xu Z. Antagonistic roles of neurofilament subunits NF-H and NF-M against NF-L in shaping dendritic arborization in spinal motor neurons. J Cell Biol. 1998; 140:1167–1176. [PubMed: 9490729]

Lacoste B, Riad M, Ratté MO, Boye SM, Lévesque D, Descarries L. Trafficking of neurokinin-1 receptors in serotonin neurons is controlled by substance P within the rat dorsal raphe nucleus. Eur J Neurosci. 2009; 29:2303–2314. [PubMed: 19490080]

Lavezzi HN, Parsley KP, Zahm DS. Mesopontine rostromedial tegmental nucleus neurons projecting to the dorsal raphe and pedunculopontine tegmental nucleus: psychostimulant-elicited Fos

expression and collateralization. Brain structure & function. 2011; 217:719–734. [PubMed: 22179106]

Lawson RP, Seymour B, Loh E, Lutti A, Dolan RJ, Dayan P, Weiskopf N, Roiser JP. The habenula encodes negative motivational value associated with primary punishment in humans. Proc Natl Acad Sci USA. 2014:201323586.

Lecourtier L, Kelly PH. A conductor hidden in the orchestra? Role of the habenular complex in monoamine transmission and cognition. Neurosci Biobehav Rev. 2007; 31:658–672. [PubMed: 17379307]

Lips EH, Gaborieau V, McKay JD, Chabrier A, Hung RJ, Boffetta P, Hashibe M, Zaridze D, Szeszenia-Dabrowska N, Lissowska J, Rudnai P, Fabianova E, Mates D, Bencko V, Foretova L, Janout V, Field JK, Liloglou T, Xinarianos G, McLaughlin J, Liu G, Skorpen F, Elvestad MB, Hveem K, Vatten L, Study E, Benhamou S, Lagiou P, Holcátová I, Merletti F, Kjaerheim K, Agudo A, Castellsagué X, Macfarlane TV, Barzan L, Canova C, Lowry R, Conway DI, Znaor A, Healy C, Curado MP, Koifman S, Eluf-Neto J, Matos E, Menezes A, Fernandez L, Metspalu A, Heath S, Lathrop M, Brennan P. Association between a 15q25 gene variant, smoking quantity and tobacco-related cancers among 17 000 individuals. Int J Epidemiol. 2010; 39:563–577. [PubMed: 19776245]

Liu R, Chang L, Wickern G. The dorsal tegmental nucleus: an axoplasmic transport study. Brain Res. 1984; 310:123–132. [PubMed: 6434154]

Liu Q, Wong-Riley MTT. Postnatal changes in tryptophan hydroxylase and serotonin transporter immunoreactivity in multiple brainstem nuclei of the rat: implications for a sensitive period. J Comp Neurol. 2010; 518:1082–1097. [PubMed: 20127812]

Liu JZ, Tozzi F, Waterworth DM, Pillai SG, Muglia P, Middleton L, Berrettini W, Knouff CW, Yuan X, Waeber G, Vollenweider P, Preisig M, Wareham NJ, Zhao JH, Loos RJF, Barroso I, Khaw K-T, Grundy S, Barter P, Mahley R, Kesaniemi A, McPherson R, Vincent JB, Strauss J, Kennedy JL, Farmer A, McGuffin P, Day R, Matthews K, Bakke P, Gulsvik A, Lucae S, Ising M, Brueckl T, Horstmann S, Wichmann H-E, Rawal R, Dahmen N, Lamina C, Polasek O, Zgaga L, Huffman J, Campbell S, Kooner J, Chambers JC, Burnett MS, Devaney JM, Pichard AD, Kent KM, Satler L, Lindsay JM, Waksman R, Epstein S, Wilson JF, Wild SH, Campbell H, Vitart V, Reilly MP, Li M, Qu L, Wilensky R, Matthai W, Hakonarson HH, Rader DJ, Franke A, Wittig M, Schäfer A, Uda M, Terracciano A, Xiao X, Busonero F, Scheet P, Schlessinger D, St Clair D, Rujescu D, Abecasis GR, Grabe HJ, Teumer A, Völzke H, Petersmann A, John U, Rudan I, Hayward C, Wright AF, Kolcic I, Wright BJ, Thompson JR, Balmforth AJ, Hall AS, Samani NJ, Anderson CA, Ahmad T, Mathew CG, Parkes M, Satsangi J, Caulfield M, Munroe PB, Farrall M, et al. Meta-analysis and imputation refines the association of 15q25 with smoking quantity. Nat Genet. 2010; 42:436–440. [PubMed: 20418889]

Manders EMM, Verbeek FJ, Aten JA. Measurement of co-localization of objects in dual3 colour confocal images. J Microsc. 1993; 169:375–382.

Marszalek JR, Williamson TL, Lee MK, Xu Z, Hoffman PN, Becher MW, Crawford TO, Cleveland DW. Neurofilament subunit NF-H modulates axonal diameter by selectively slowing neurofilament transport. J Cell Biol. 1996; 135:711–724. [PubMed: 8909545]

Matsumoto M, Hikosaka O. Lateral habenula as a source of negative reward signals in dopamine neurons. Nature. 2007; 447:1111–1115. [PubMed: 17522629]

Matsumoto M, Hikosaka O. Representation of negative motivational value in the primate lateral habenula. Nat Neurosci. 2009; 12:77–84. [PubMed: 19043410]

Morris JS, Smith KA, Cowen PJ, Friston KJ, Dolan RJ. Covariation of activity in habenula and dorsal raphé nuclei following tryptophan depletion. Neuroimage. 1999; 10:163–172. [PubMed: 10417248]

Neckers LM, Schwartz JP, Wyatt RJ, Speciale SG. Substance P afferents from the habenula innervate the dorsal raphe nucleus. Exp Brain Res. 1979; 37:619–623. [PubMed: 520447]

Olucha-Bordonau FE, Teruel V, Barcia-González J, Ruiz-Torner A, Valverde-Navarro AA, Martínez-Soriano F. Cytoarchitecture and efferent projections of the nucleus incertus of the rat. J Comp Neurol. 2003; 464:62–97. [PubMed: 12866129]

Park MR. Monosynaptic inhibitory postsynaptic potentials from lateral habenula recorded in dorsal raphe neurons. Brain Res Bull. 1987; 19:581–586. [PubMed: 3690368]

Paxinos, G.; Watson, C. The Rat Brain in Stereotaxic Coordinates. 6. New York: Elsevier/Academic Press; 2006.

Paxinos, G. The Rat Nervous System. 3. New York: Elsevier/Academic Press; 2004.

Quina LA, Wang S, Ng L, Turner EE. Brn3a and Nurr1 mediate a gene regulatory pathway for habenula development. J Neurosci. 2009; 29:14309–14322. [PubMed: 19906978]

Ranft K, Dobrowolny H, Krell D, Bielau H, Bogerts B, Bernstein H-G. Evidence for structural abnormalities of the human habenular complex in affective disorders but not in schizophrenia. Psychol Med. 2010; 40:557–567. [PubMed: 19671211]

Ren J, Qin C, Hu F, Tan J, Qiu L, Zhao S, Feng G, Luo M. Habenula "cholinergic" neurons co-release glutamate and acetylcholine and activate postsynaptic neurons via distinct transmission modes. Neuron. 2011; 69:445–452. [PubMed: 21315256]

Reisine TD, Soubrie P, Artaud F, Glowinski J. Involvement of lateral habenula-dorsal raphe neurons in the differential regulation of striatal and nigral serotonergic transmission cats. J Neurosci. 1982; 2:1062–1071. [PubMed: 6180148]

Roiser JP, Levy J, Fromm SJ, Nugent AC, Talagala SL, Hasler G, Henn FA, Sahakian BJ, Drevets WC. The effects of tryptophan depletion on neural responses to emotional words in remitted depression. Biol Psychiatry. 2009; 66:441–450. [PubMed: 19539268]

Salas R, Sturm R, Boulter J, de Biasi M. Nicotinic receptors in the habenulo-interpeduncular system are necessary for nicotine withdrawal in mice. J Neurosci. 2009; 29:3014–3018. [PubMed: 19279237]

Salas R, Baldwin P, de Biasi M, Montague PR. BOLD Responses to Negative Reward Prediction Errors in Human Habenula. Front Hum Neurosci. 2010; 4:36. [PubMed: 20485575]

Sartorius A, Henn FA. Deep brain stimulation of the lateral habenula in treatment resistant major depression. Med Hypotheses. 2007; 69:1305–1308. [PubMed: 17498883]

Sartorius A, Kiening KL, Kirsch P, von Gall CC, Haberkorn U, Unterberg AW, Henn FA, Meyer-Lindenberg A. Remission of major depression under deep brain stimulation of the lateral habenula in a therapy-refractory patient. Biol Psychiatry. 2010; 67:e9–e11. [PubMed: 19846068]

Sego C, Gonçalves L, Lima L, Furigo IC, Donato J, Metzger M. The lateral habenula and the rostromedial tegmental nucleus innervate neurochemically distinct subdivisions of the dorsal raphe nucleus in the rat. J Comp Neurol. 2014; 522:1454–1484. [PubMed: 24374795]

Sevigny CP, Bassi J, Williams DA, Anderson CR, Thomas WG, Allen AM. Efferent projections of C3 adrenergic neurons in the rat central nervous system. J Comp Neurol. 2012; 520:2352–2368. [PubMed: 22237784]

Shabel SJ, Proulx CD, Trias A, Murphy RT, Malinow R. Input to the lateral habenula from the basal ganglia is excitatory, aversive, and suppressed by serotonin. Neuron. 2012; 74:475–481. [PubMed: 22578499]

Sharp PE, Turner-Williams S, Tuttle S. Movement-related correlates of single cell activity in the interpeduncular nucleus and habenula of the rat during a pellet-chasing task. Behav Brain Res. 2006; 166:55–70. [PubMed: 16143407]

Sheffield EB, Quick MW, Lester RA. Nicotinic acetylcholine receptor subunit mRNA expression and channel function in medial habenula neurons. Neuropharmacology. 2000; 39:2591–2603. [PubMed: 11044729]

Shumake J, Gonzalez-Lima F. Functional opposition between habenula metabolism and the brain reward system. Front Hum Neurosci. 2013; 7:662. [PubMed: 24133441]

Sim LJ, Joseph SA. Dorsal raphe nucleus efferents: termination in peptidergic fields. Peptides. 1993; 14:75–83. [PubMed: 8441710]

Stamatakis AM, Stuber GD. Activation of lateral habenula inputs to the ventral midbrain promotes behavioral avoidance. Nature neuroscience. 2012; 15:1105–1107.

Sternberger LA, Harwell LW, Sternberger NH. Neurotypy: regional individuality in rat brain detected by immunocytochemistry with monoclonal antibodies. Proc Natl Acad Sci USA. 1982; 79:1326–1330. [PubMed: 7041117]

Stopper CM, Floresco SB. What's better for me? Fundamental role for lateral habenula in promoting subjective decision biases. Nature neuroscience. 2013; 17:33–35.

Takamori S, Rhee JS, Rosenmund C, Jahn R. Identification of a vesicular glutamate transporter that defines a glutamatergic phenotype in neurons. Nature. 2000; 407:189–194. [PubMed: 11001057]

Takamori S, Rhee JS, Rosenmund C, Jahn R. Identification of differentiation-associated brain-specific phosphate transporter as a second vesicular glutamate transporter (VGLUT2). J Neurosci. 2001; 21:RC182. [PubMed: 11698620]

Tapper AR, McKinney SL, Nashmi R, Schwarz J, Deshpande P, Labarca C, Whiteaker P, Marks MJ, Collins AC, Lester HA. Nicotine activation of alpha4* receptors: sufficient for reward, tolerance, and sensitization. Science. 2004; 306:1029–1032. [PubMed: 15528443]

Ullsperger M, von Cramon DY. Error monitoring using external feedback: specific roles of the habenular complex, the reward system, and the cingulate motor area revealed by functional magnetic resonance imaging. J Neurosci. 2003; 23:4308–4314. [PubMed: 12764119]

Valentino RJ, Bey V, Pernar L, Commons KG. Substance P Acts through Local Circuits within the Rat Dorsal Raphe Nucleus to Alter Serotonergic Neuronal Activity. J Neurosci. 2003; 23:7155–7159. [PubMed: 12904475]

Vincent SR, Staines WA, McGeer EG, Fibiger HC. Transmitters contained in the efferents of the habenula. Brain Res. 1980; 195:479–484. [PubMed: 6156737]

Viswanath H, Carter AQ, Baldwin PR, Molfese DL, Salas R. The medial habenula: still neglected. Front Hum Neurosci. 2013; 7:931. [PubMed: 24478666]

Wagner F, Stroh T, Veh RW. Correlating habenular subnuclei in rat and mouse using topographical, morphological and cytochemical criteria. J Comp Neurol. 2014

Wang RY, Aghajanian GK. Physiological evidence for habenula as major link between forebrain and midbrain raphe. Science. 1977; 197:89–91. [PubMed: 194312]

Ware JJ, van den Bree MBM, Munafò MR. Association of the CHRNA5-A3-B4 gene cluster with heaviness of smoking: a meta-analysis. Nicotine Tob Res. 2011; 13:1167–1175. [PubMed: 22071378]

Weissner W, Winterson BJ, Stuart-Tilley A, Devor M, Bove GM. Time course of substance P expression in dorsal root ganglia following complete spinal nerve transection. J Comp Neurol. 2006; 497:78–87. [PubMed: 16680762]

Wojcik SM, Rhee JS, Herzog E, Sigler A, Jahn R, Takamori S, Brose N, Rosenmund C. An essential role for vesicular glutamate transporter 1 (VGLUT1) in postnatal development and control of quantal size. Proc Natl Acad Sci USA. 2004; 101:7158–7163. [PubMed: 15103023]

Wouterlood FG, Härtig W, Groenewegen HJ, Voorn P. Density gradients of vesicular glutamate- and GABA transporter-immunoreactive boutons in calbindinand μ-opioid receptor-defined compartments in the rat striatum. Journal of Comparative Neurology. 2012; 520:2123–2142. [PubMed: 22173881]

Yang L-M, Hu B, Xia Y-H, Zhang B-L, Zhao H. Lateral habenula lesions improve the behavioral response in depressed rats via increasing the serotonin level in dorsal raphe nucleus. Behav Brain Res. 2008; 188:84–90. [PubMed: 18054396]

Zhao-Shea R, Liu L, Pang X, Gardner PD, Tapper AR. Activation of GABAergic neurons in the interpeduncular nucleus triggers physical nicotine withdrawal symptoms. Curr Biol. 2013; 23:2327–2335. [PubMed: 24239118]

Zhou J, Nannapaneni N, Shore S. Vessicular glutamate transporters 1 and 2 are differentially associated with auditory nerve and spinal trigeminal inputs to the cochlear nucleus. J Comp Neurol. 2007; 500:777–787. [PubMed: 17154258]

Zinchuk V, Grossenbacher-Zinchuk O. Quantitative colocalization analysis of fluorescence microscopy images. Curr Protoc Cell Biol. 2014; 62:4.19.1–4.19.14.

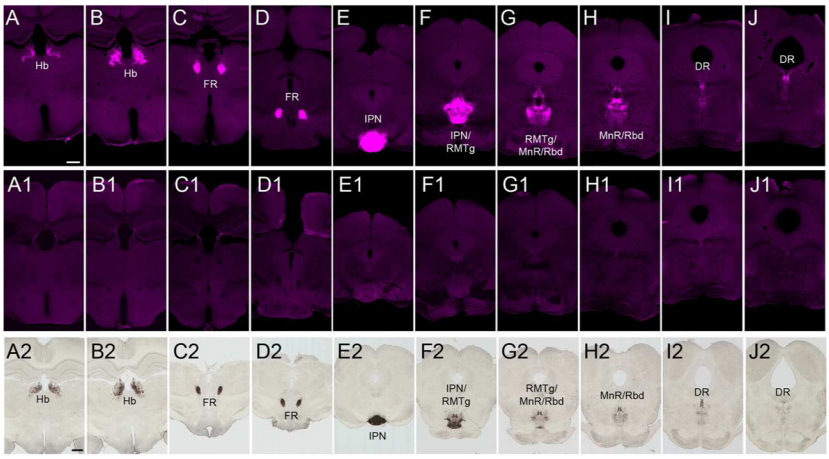

Figure 1. GPR151 is localized in habenular axonal projections in rat and mouse brain

Coronal brain sections of wildtype mouse (A–J) and rat (A2–J2) showing restricted expression of GPR151 in habenula (A–B, A2–B2), fasciculus retroflexus (C–D, C2–D2), interpeduncular nucleus (E–F, E2–F2), rostromedial tegmental nucleus (F–G, F2–G2), median and paramedian raphe (F–H, F2–H2), rhabdoid nucleus (F–H, F2–H2) and dorsal raphe (I–J, I2–J2). GPR151 immunoreactivity is completely absent in *Gpr151*$^{-/-}$ mice (A1–J1). Scale bar: 500 μm in A–J, 1000μm in A2–J2.

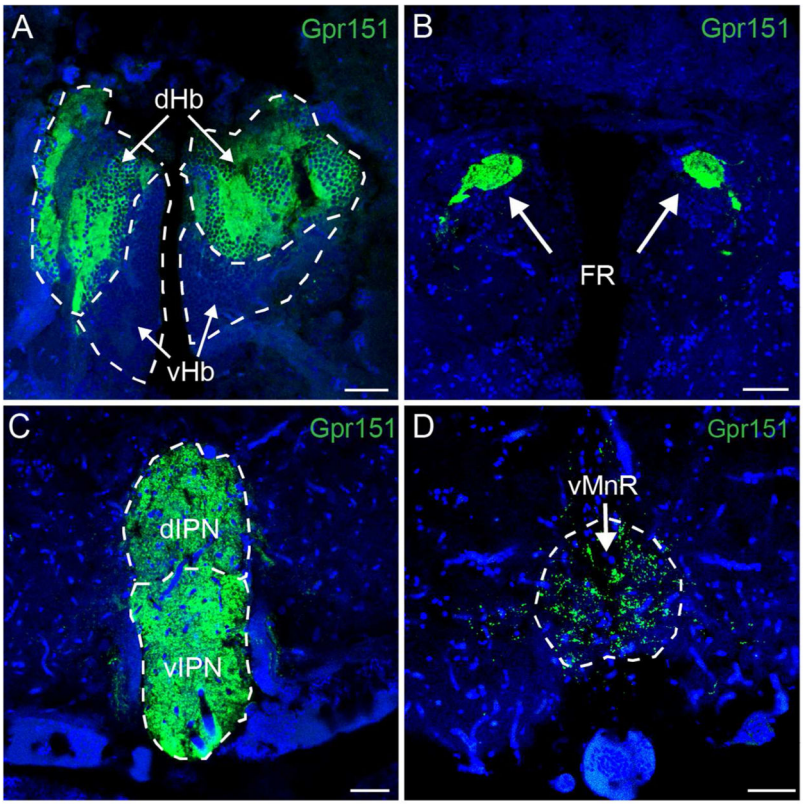

Figure 2. GPR151 is expressed in the habenular circuitry of zebrafish

Immunohistochemistry of coronal brain sections of adult zebrafish using a rabbit polyclonal antibody against human GPR151 yielded selective labeling of habenular axons projecting from the habenula (A), through the FR (B) to the dIPN and vIPN (C) as well as to the ventral median raphe (D). DAPI nuclear stain is shown in blue. Scale bar: 50μm.

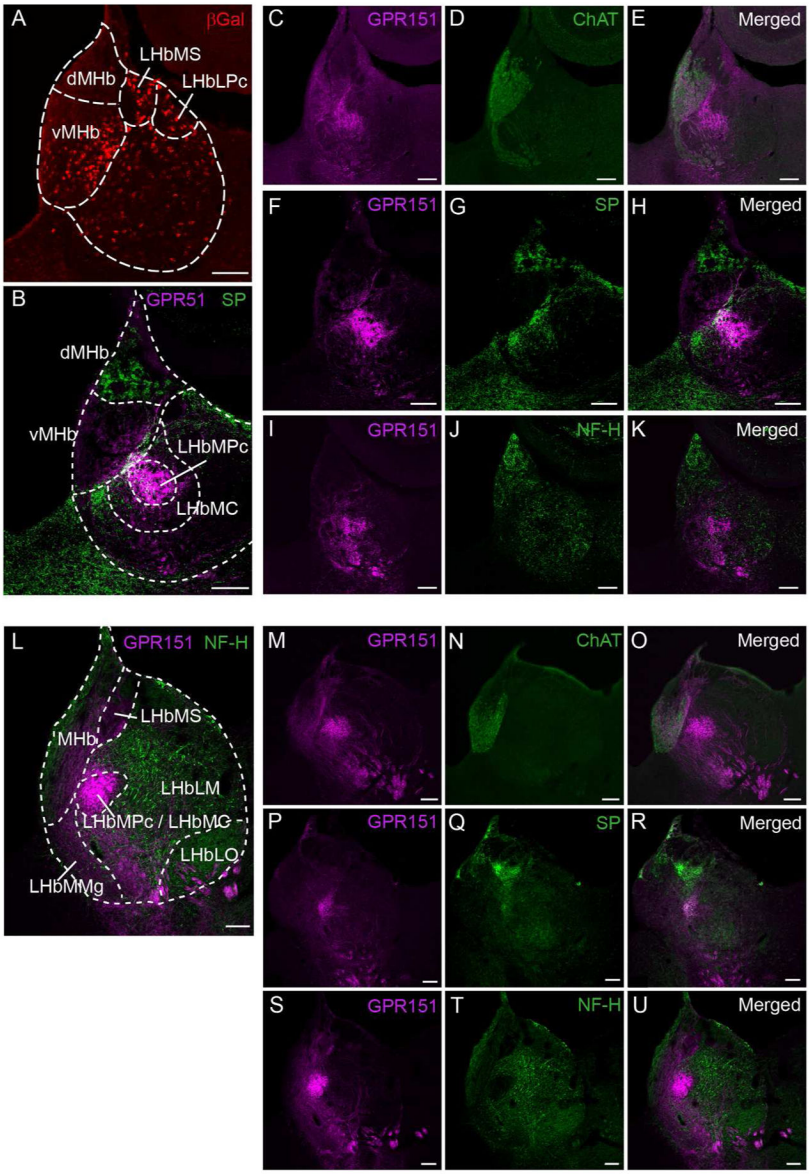

Figure 3. GPR151 labels specific subpopulations of medial and lateral habenula neurons

A: Coronal section of the habenula of *Gpr151*$^{-/-}$ mice showing immunostaining for the β-galactosidase reporter contained in the *Gpr151* gene deletion vector employed to generate *Gpr151*$^{-/-}$ mice. β-galactosidase positive cells are located mainly in the vMHb and the dorsal part of the LHb. B–K: Coronal sections of the wildtype mouse habenula showing immunostaining for GPR151 (magenta in B,C,E,F,H,I,K) relative to the immunostaining for acetylcholine transferase (ChAT, green in D,E), substance P (SP, green in B,G,H) and neurofilament-H (NF-H, green in J,K). L–U: Coronal sections of rat mouse habenula showing immunostaining for GPR151 (magenta in L,M,O,P,R,S,U) relative to the immunostaining for ChAT (green in N,O), SP (green in Q,R) and NF-H (green in L,T,U). In the LHb, GPR151 is mainly expressed in the LHbMPc and LHbMC subnuclei. In the MHb, GPR151 is expressed in the cholinergic vMHb, but not in the SP expressing dMHb. Scale bar: 100 μm.

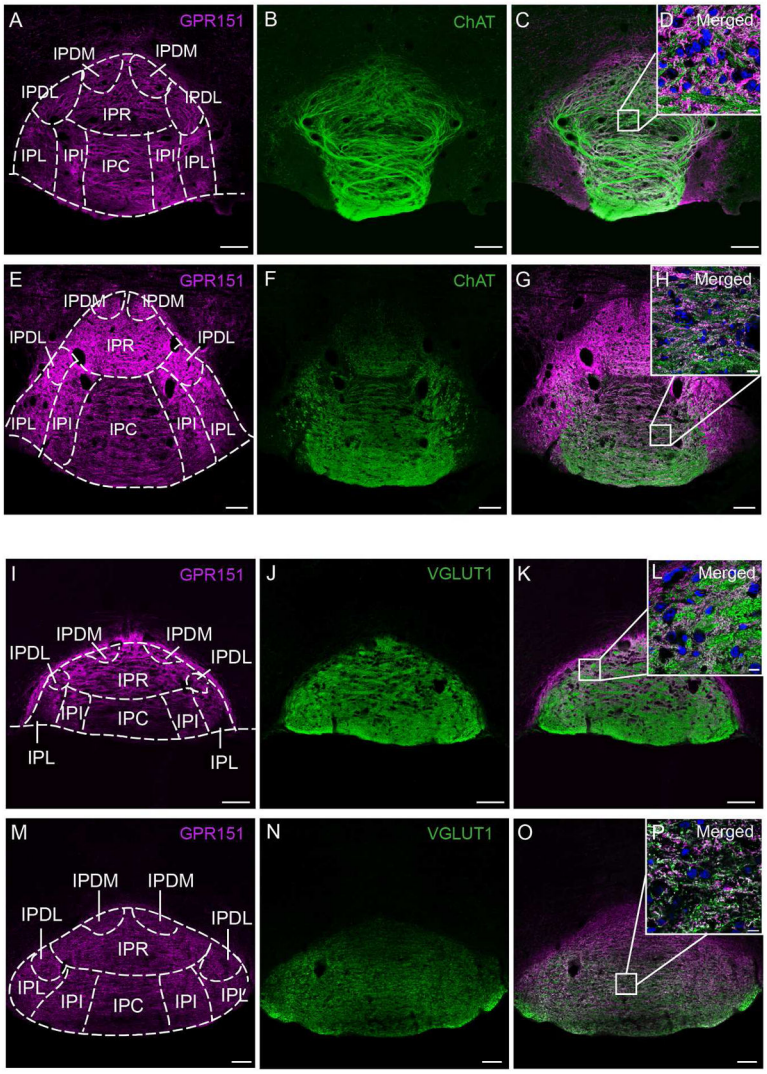

Figure 4. GPR151 immunoreactive habenular neurons project to the interpeduncular nucleus

Coronal sections of the interpeduncular nucleus of mouse (A–D, I–L) and rat (E–H, M–P) showing immunostaining for GPR151 (magenta in A,C,D,E,G,H,I,K,L,M,O,P) relative to the immunostaining for acetylcholine transferase (ChAT, green in B–D, F–H) and vesicular glutamate transporter 1 (VGLUT1, green in J–L,N–P). Colocalization of GPR151 and ChAT and GPR151 and VGLUT1 is observed in the rostral and central part of the IPN. Scale bar: 100 μm. D,H,L,P are higher magnifications of the boxed areas in the inset of each panel. DAPI nuclear stain is shown in blue. Scale bar: 10 μm.

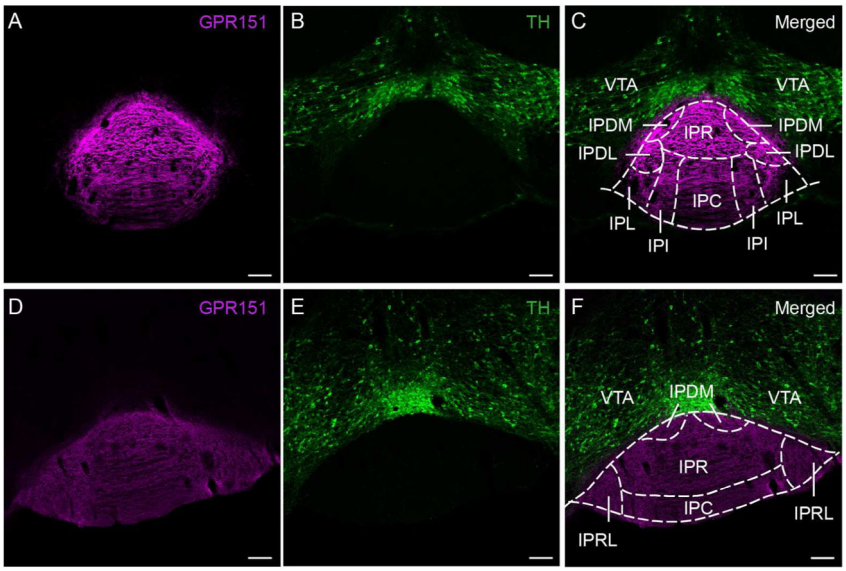

Figure 5. GPR151 habenular neurons do not project to the ventral tegmental area

Coronal sections of mouse (A–C) and rat (D–F) in the IPN and ventral tegmental area showing immunostaining for GPR151 (magenta in A,C,D,F) relative to the immunostaining for tyrosine hydroxylase (TH, green in B–C,E–F). GPR151 immunostaining is observed in the IPN but not in the ventral tegmental area. Scale bar: 100 μm.

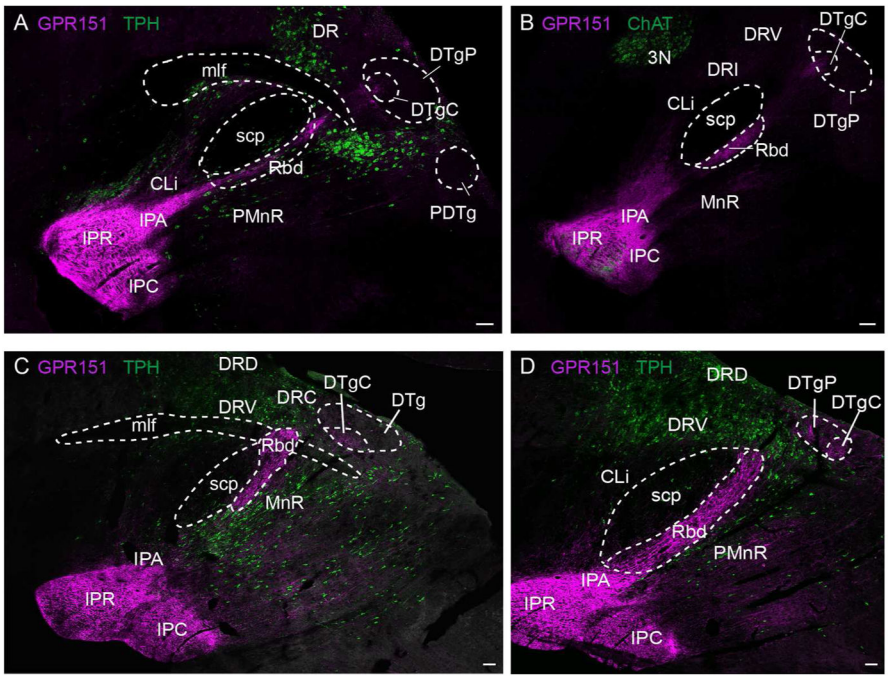

Figure 6. GPR151 habenular neurons project to the IPN, dorsal tegmental nucleus and mesencephalic raphe nuclei

Sagittal sections of mouse (A–B) and rat (C–D) in the midbrain and pons showing GPR151 immunostaining (magenta in A–D) relative to the immunostaining for tryptophan hydroxylase (TPH, green in A,C,D) or ChAT (green in B). GPR151 habenular neurons project to the IPN, the rhabdoid nucleus, the dorsal tegmental nucleus and the mesencephalic raphe nuclei. ChAT immunostaining is observed in the IPN and the oculomotor nucleus. TPH immunostaining labels the serotonergic neurons in the mesencephalic raphe nuclei. Scale bar: 100μm.

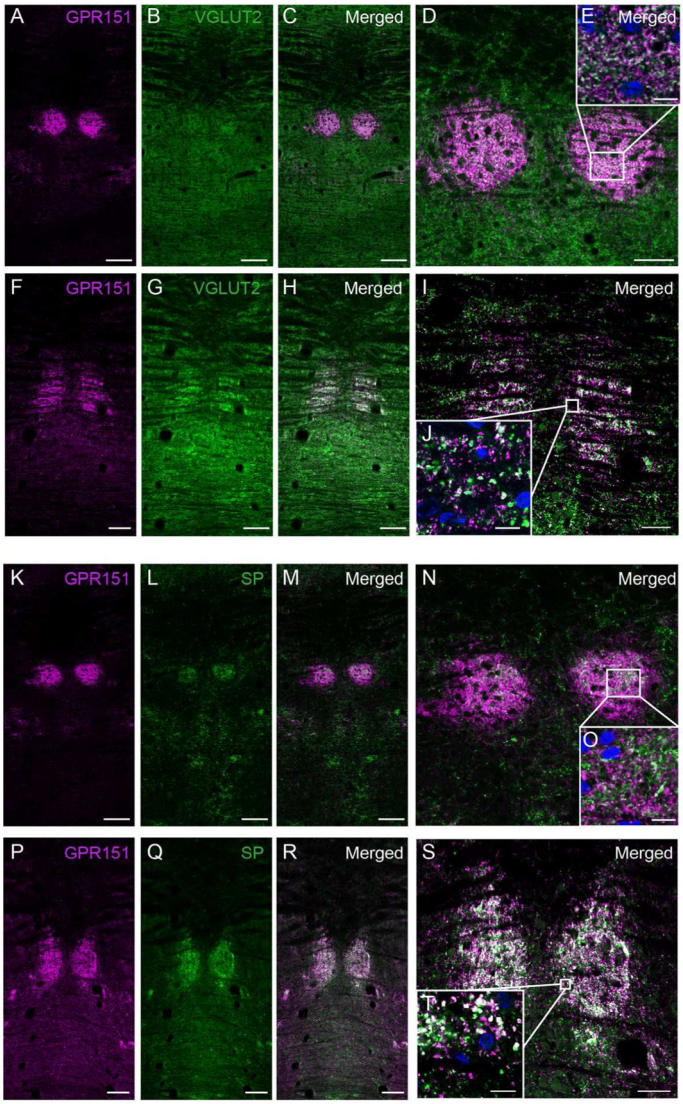

Figure 7. GPR151, substance P and VGLUT2 expression in the rhabdoid nucleus

Coronal sections of mouse (A–E, K–O) and rat (F–J, P–T) through the rhabdoid nucleus. GPR151 immunoreactivity is shown in magenta. Vesicular glutamate transporter 2 immunoreactivity is shown in green in B–E and G–J. Substance P immunoreactivity is shown in green in L–O and Q–T. E, J, O and T are higher magnifications of the boxed areas. DAPI nuclear stain is shown in blue. Colocalization of GPR151 and VGLUT2 as well as GPR151 and substance P is observed in the rhabdoid nucleus. Scale bar: 100μm in A–C, F–H, K–M, P–R; 50μm in D, I, N, S; 10μm in E, J, O, T.

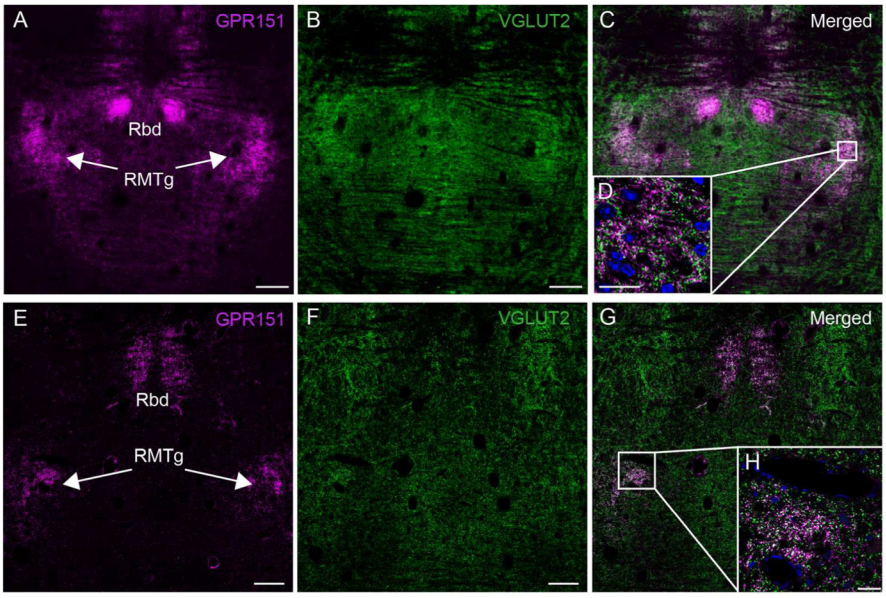

Figure 8. GPR151 immunoreactive habenular neurons project to the rostromedial tegmental nucleus

Coronal sections of mouse (A–D) and rat (E–H) in the midbrain showing GPR151 immunostaining (magenta in A,C,D,E,G,H) relative to the immunostaining for vesicular glutamate transporter 2 (VGLUT2, green in B–D,F–H). GPR151 immunostaining is observed in the rostromedial tegmental nucleus and rhabdoid nucleus. D,H are higher magnifications of the boxed areas in the inset of each panel. Colocalization of GPR151 and VGLUT2 is observed in the RMTg. DAPI nuclear stain is shown in blue. Scale bar: 100 μm in A–C, E–G; 10μm in D,H.

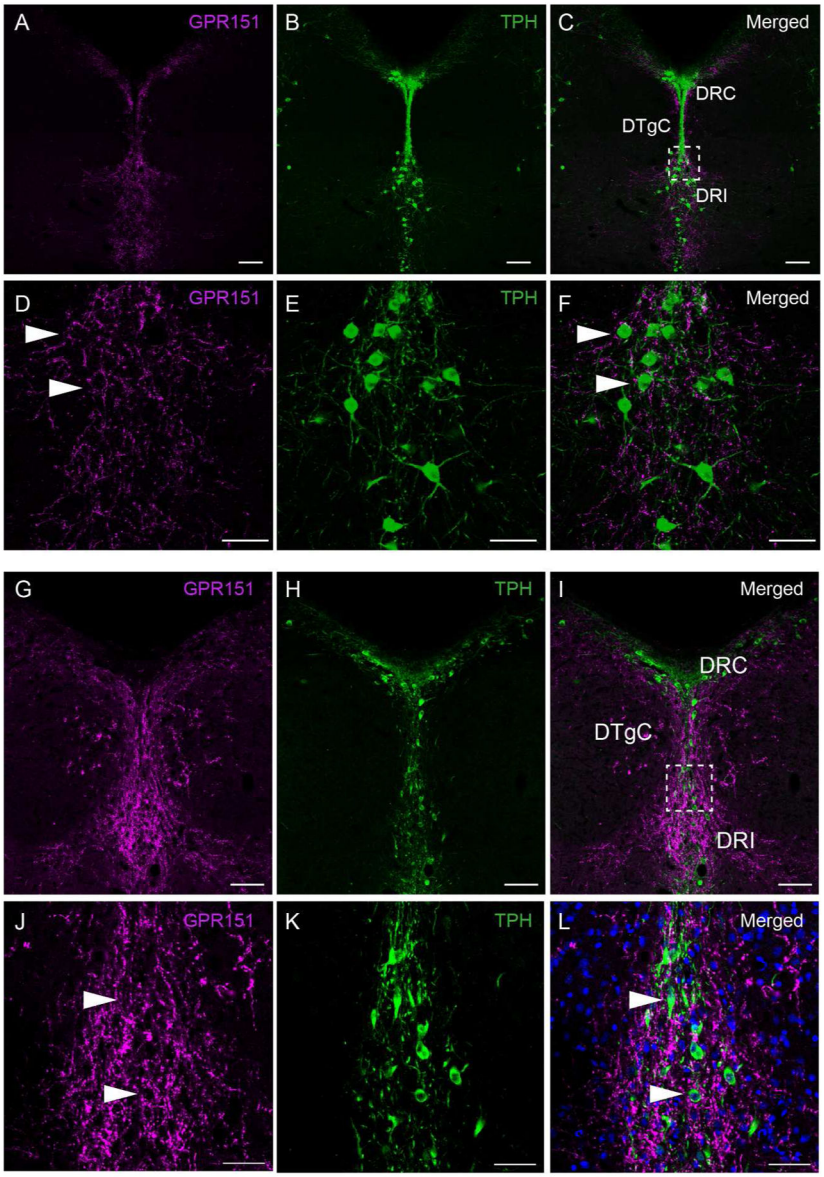

Figure 9. GPR151 expression in the caudal dorsal raphe nucleus

Coronal sections of mouse (A–F) and rat (G–L) through the caudal dorsal raphe nucleus. GPR151 immunoreactivity is shown in magenta and tryptophan hydroxylase (TPH) immunoreactivity is shown in green. DAPI nuclear stain is shown in blue. Panels D–F are magnifications of the boxed area in C. Panels J–L are magnifications of the boxed area in I. GPR151 positive fibers make close contact to serotonergic neurons (arrows). Scale bar: 100μm in A–C, G–I; 50μm in D–F, J–L.

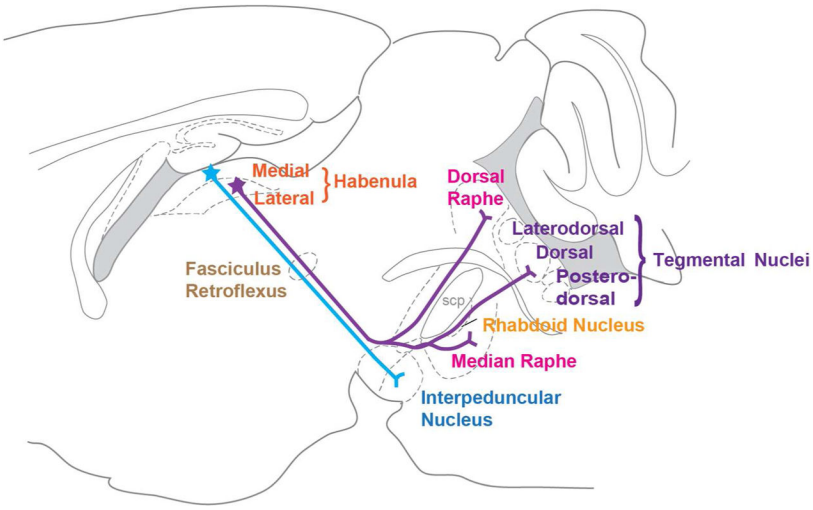

Figure 10. Schematic representation of GPR151 expressing habenular projections

Schematic sagittal view of a rodent brain depicting GPR151 expressing habenular projections. A prominent GPR151 positive projection arises in the ventral medial habenula and terminates in the interpeduncular nucleus (blue). From the lateral habenula, GPR151 immunoreactive axonal fibers project toward the interpeduncular nucleus, then travel through or adjacent to it, and then continue in a dorsal-caudal direction. The lateral habenular fibers travel both dorsally and ventrally to the superior cerebellar peduncle and terminate in the rostromedial tegmental nucleus, rhabdoid nucleus, dorsal tegmental nucleus as well as the median, paramedian and dorsal raphe nuclei.

J Comp Neurol. Author manuscript; available in PMC 2016 February 15.

Table 1

Primary antibodies

Antibody target	Immunogen	Manufacturer, cat. no, species	RRID	Working concentration or dilution
GPR151	Synthetic peptide derived from C-terminal of human GPR151 (aa 370–419, *EKEKPSSPSSGKGKTEKAEIPILPDVEQFWHERDTVPSVQDNDPIPWEHEDQETGEGVK*)	Sigma, SAB4500418, rabbit polyclonal	AB_10743815	0.2μg/ml (rat and mouse), 0.1μg/ml (zebrafish)
GPR151	Full length human GPR151 protein	Sigma, SAB1402000, mouse polyclonal	AB_10608138	0.5μg/ml (rat and mouse), 1μg/ml (zebrafish)
β-galactosidase	Full length native *ESCHERICHIA COLI* protein	Abcam, AB9361, chicken polyclonal	AB_307210	2μg/ml
Vesicular glutamate transporter 1 (VGLUT1)	Strep-Tag® fusion protein of rat VGLUT 1 (amino acids 456 – 560, *TLSGMVCPIIVGAMT*).	Synaptic Systems, 135303, rabbit polyclonal	AB_887876	1μg/ml
Vesicular glutamate transporter 1 (VGLUT1)	Purified recombinant protein of rat VGLUT 1 (amino acids 456 – 560, *TLSGMVCPIIVGAMT*).	Synaptic Systems, 135304, guinea pig polyclonal	AB_887878	1:1000
Vesicular glutamate transporter 2 (VGLUT2)	Strep-Tag® fusion protein of rat VGLUT 2 (amino acids 510 – 582, *EKQPWADPEETSEEKCGFIHEDELDEETGDITQNYINYGTTKSYGATSQENGGWPNGEKKEEFVQESAQDAYSYKDRDDYS*).	Synaptic Systems, 135403, rabbit polyclonal	AB_887883	1μg/ml
Vesicular glutamate transporter 2 (VGLUT2)	Purified recombinant protein of rat VGLUT 2 (amino acids 510 – 582, *EKQPWADPEETSEEKCGFIHEDELDEETGDITQNYINYGTTKSYGATSQENGGWPNGEKKEEFVQESAQDAYSYKDRDDYS*).	Synaptic Systems, 135404, guinea pig polyclonal	AB_887884	1:1000
Choline acetyltransferase (ChAT)	Human placental choline acetyltransferase enzyme	Millipore, AB144P, goat polyclonal	AB_2079751	2μg/ml
Neurofilament H - non phosphorylated	Homogenized hypothalami from Fischer 344 rat brain	Covance, SMI-32R, mouse monoclonal (clone SMI-32)	AB_10123643	1:4000 (rat), 1:1000 (mouse)
Tyrosine hydroxylase (TH)	Rat tyrosine hydroxylase	Sigma, T1299 mouse monoclonal (clone TH-2)	AB_477560	1:500
Tryptophan hydroxylase (TPH)	Recombinant rabbit tryptophan hydroxylase	Sigma, T0678, mouse monoclonal (clone WH-3)	AB_261587	2μg/ml
Tryptophan hydroxylase (TPH)	Recombinant rabbit tryptophan hydroxylase	Chemicon, AB1541, sheep polyclonal	AB_90754	0.4μg/ml
Substance P	Synthetic substance P coupled to keyhole limpet hemocyanin with carbodiimide	Immunostar, 20064, rabbit polyclonal	AB_572266	1:1000
Substance P	Eight amino acids of the COOH-terminal fragment of substance P (NC1/34HL)	Santa Cruz, sc-21715, rat monoclonal	AB_628299	0.8μg/ml

Table 2

Secondary antibodies

Target species	Produced in	Conjugation	Manufacturer, cat. no	Working concentration
Rabbit	Goat	Cy3	Jackson ImmunoResearch, 111-166-003	3μg/ml
Mouse	Goat	Alexa 488	Jackson ImmunoResearch, 115-545-003	3μg/ml
Mouse	Goat	DyLight 650	Nordic BioSite, IR-GTMU-003F650	5μg/ml
Mouse	Donkey	Cy5	Jackson ImmunoResearch, 711-175-152	3μg/ml
Mouse	Horse	Biotin	Vector Laboratories, BA-2000	3μg/ml
Rabbit	Donkey	Alexa 488	Jackson ImmunoResearch, 711-545-152	3μg/ml
Mouse	Donkey	Cy3	Jackson ImmunoResearch, 715-165-150	3μg/ml
Sheep	Donkey	Cy3	Jackson ImmunoResearch, 713-165-147	3μg/ml
Goat	Donkey	DyLight 549	Jackson ImmunoResearch, 705-505-147	3μg/ml
Rat	Donkey	Alexa 647	Jackson ImmunoResearch, 712-605-153	3μg/ml
Guinea pig	Donkey	Cy3	Jackson ImmunoResearch, 706-165-148	3μg/ml